

34  
/TEMPERATURE EFFECTS ON ACTIVATED  
CARBON ADSORPTION IN FIXED-BEDS/

by

IE-HONG LIN

B.E., National Cheng Kung University  
Taiwan, R.O.C. , 1980

---

A MASTER'S THESIS

submitted in partial fulfillment of the  
requirements for the degree

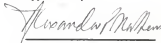
MASTER OF SCIENCE

Department of Civil Engineering

KANSAS STATE UNIVERSITY  
Manhattan, Kansas

1985

Approved by :



Major Professor

LD  
2668  
.74  
1965  
L56  
c. 2

ALL202 644908

TABLE OF CONTENTS

	Page
LIST OF TABLES .....	iii
LIST OF FIGURES .....	iv
NOTATIONS .....	vi
CHAPTER 1 INTRODUCTION .....	1
1-1 General Discussion .....	1
1-2 Objectives and Scopes of the Research .....	7
CHAPTER 2 REVIEW OF RELATED LITERATURE .....	9
2-1 Single Solute Adsorption Models .....	9
2-1-1 Equilibrium Models .....	9
2-1-2 Batch Kinetic Models .....	12
2-1-3 Fixed Bed Models .....	17
2-2 Multicomponent Adsorption Models .....	20
2-2-1 Equilibrium Models .....	20
2-2-2 Batch Kinetic Models .....	22
2-2-3 Fixed Bed Models .....	23
2-3 Factors Influencing Adsorption .....	24
2-3-1 Temperature .....	24
2-3-2 Other factors .....	27
CHAPTER 3 EXPERIMENTAL MATERIALS AND METHODS .....	29
3-1 Materials .....	29
3-1-1 Adsorbents .....	29
3-1-2 Adsorbates .....	31
3-2 Methods .....	33
3-2-1 Analytical Methods .....	33
3-2-2 Equilibrium Experiments .....	36
3-2-3 Batch Kinetic Experiments .....	38
3-2-4 Fixed Bed Experiments .....	41

CHAPTER 4 SINGLE SOLUTE ADSORPTION .....	44
4-1 Equilibrium Studies .....	44
4-2 Batch Kinetic Studies .....	59
4-3 Fixed-Bed Studies .....	72
CHAPTER 5 MULTICOMPONENT ADSORPTION .....	86
5-1 Equilibrium Studies .....	86
5-2 Batch Kinetic Studies .....	96
5-3 Fixed bed Studies .....	104
CHAPTER 6 CONCLUSIONS AND RECOMMENDATIONS .....	107
6-1 Conclusions .....	107
6-2 Recommendations .....	109
REFERENCES .....	110

## LIST OF TABLES

Table	page
1.1 Reported Maximum Concentrations of Phenol in Industrial Effluents .....	5
1.2 Reported Maximum Concentrations of Chlorophenol in Industrial Effluents .....	6
3.1 Properties of Activated Carbon .....	30
3.2 Adsorbates and Their Properties .....	32
3.3 Molar Absorptivities of Adsorbates (l/mole-cm) .....	35
4.1 Isotherm Parameters for Phenol and PCP .....	46
4.2 Adsorption Equilibrium Constants for a Range of Temperature .....	47
4.3 Isotherm Parameters for Phenol and PCP Calculated from Equations 4.2 through 4.4 .....	48
4.4 Solid Phase Diffusion Coefficients and Film Transfer Coefficients for Phenol and PCP .....	63
4.5 Solid Phase Diffusion Coefficients and Film Transfer Coefficients of Solutes Calculated from Equation 4.8 through 4.11 .....	64
4.6 Operating Data for Fixed Bed Experiments at 20°C .....	74
4.7 Operating Data for Fixed Bed Experiments at 35°C .....	75
4.8 Operating Data for Fixed Bed Experiments : Step Change from 20° to 35°C after 3 hrs .....	76
4.9 Operating Data for Fixed Bed Experiments : Step Change from 35° to 20°C after 3 hrs .....	77
5.1 Multicomponent Equilibrium for Phenol and PCP at 20°C by Mathews' Equilibrium Model.....	88
5.2 Multicomponent Equilibrium for Phenol and PCP at 20°C by Prausnitz's Equilibrium Model .....	89
5.3 Multicomponent Equilibrium for Phenol and PCP at 35°C by Mathews' Equilibrium Model .....	90
5.4 Multicomponent Equilibrium for Phenol and PCP at 35°C by Prausnitz's Equilibrium Model .....	91

## LIST OF FIGURES

Figure	Page
2.1 Adsorption on Porous Adsorbent - Rate Limiting Mechanisms .....	13
3.1 Schematic of Batch Kinetic System .....	40
3.2 Schematic of the Fixed Bed Adsorption System .....	43
4.1 Adsorption Isotherm for Phenol at 20°C .....	49
4.2 Adsorption Isotherm for Phenol at 25°C .....	50
4.3 Adsorption Isotherm for Phenol at 30°C .....	51
4.4 Adsorption Isotherm for Phenol at 35°C .....	52
4.5 Adsorption Isotherm for PCP at 20°C .....	53
4.6 Adsorption Isotherm for PCP at 25°C .....	54
4.7 Adsorption Isotherm for PCP at 30°C .....	55
4.8 Adsorption Isotherm for PCP at 35°C .....	56
4.9 Adsorption Isosteres for Determining Isosteric Heat of Adsorption .....	57
4.10 Isosteric Heat of Adsorption $Q_{st,a}$ plotted against Amount Adsorbed $q$ .....	58
4.11 Adsorption Rate for Phenol at 20°C and 25°C .....	65
4.12 Adsorption Rate for Phenol at 30°C and 35°C .....	66
4.13 Adsorption Rate for PCP at 20°C and 25°C .....	67
4.14 Adsorption Rate for PCP at 30°C and 35°C .....	68
4.15 $k_f$ and $D_e$ values versus $T$ following Arrhenius' law .....	69
4.16 Adsorption Rates for Phenol for Step Change from 20°C to 35°C and from 35°C to 20°C after 1 hr .....	70
4.17 Adsorption Rates for PCP for Step Change from 20°C to 35°C and from 35°C to 20°C after 1 hr .....	71
4.18 Breakthrough Curves for Phenol at 20°C .....	78
4.19 Breakthrough Curves for Phenol at 35°C .....	79

4.20 Breakthrough Curves for PCP at 20°C .....	80
4.21 Breakthrough Curves for PCP at 35°C .....	81
4.22 Breakthrough Curves for Phenol for Step Change from 20° to 35°C after 3 hre .....	82
4.23 Breakthrough Curves for Phenol for Step Change from 35°C to 20°C after 3 hre .....	83
4.24 Breakthrough Curves for PCP for Step Change from 20°C to 35°C after 3 hre .....	84
4.25 Breakthrough Curves for PCP for Step Change from 35°C to 20°C after 3 hrs .....	85
5.1 Phenol in Multicomponent Isotherm at 20°C .....	92
5.2 PCP in Multicomponent Isotherm at 20°C .....	93
5.3 Phenol in Multicomponent Isotherm at 35°C .....	94
5.4 PCP in Multicomponent Isotherm at 35°C .....	95
5.5 Adsorption Rate for (Phenol+PCP) at 20°C with Mathewe' Equilibrium Model .....	98
5.6 Adsorption Rate for (Phenol+PCP) at 20°C with Prausnitz's Equilibrium Model .....	99
5.7 Adsorption Rate for (Phenol+PCP) at 35°C with Mathewe' Equilibrium Model .....	100
5.8 Adsorption Rate for (Phenol+PCP) at 35°C with Prausnitz's Equilibrium Model .....	101
5.9 Adsorption Rate for (Phenol+PCP) for Step Change from 20° to 35°C with Prausnitz's Equilibrium Model .....	102
5.10 Adsorption Rate for (Phenol+PCP) for Step Change from 35° to 20°C with Prausnitz's Equilibrium Model .....	103
5.11 Breakthrough Curves for (Phenol+PCP) for Step Change from 20° to 35°C after 3 hre .....	105
5.12 Breakthrough Curves for (Phenol+PCP) for Step Change from 35° to 20°C after 3 hre .....	106

## NOTATIONS

A	Isotherm parameter
$A_p$	surface area of particle
B	Isotherm parameter
$\beta$	Isotherm parameter
$C_e$	solute concentration
C	solute concentration in the liquid phase
$\bar{C}$	reduced solute concentration, $C/C_0$
$C_e$	solute concentration at equilibrium
$C_s$	solute concentration at particle surface
$\bar{C}_s$	reduced solute concentration at particle surface, $C_s/C_0$
$C_0$	Initial concentration
$D_s$	solid phase diffusion coefficient
$D_g$	solute distribution number
$E_d$	surface diffusion modulus
$\epsilon$	adsorber void fraction
K	isotherm parameter
$k_f$	film transfer coefficient
$L_b$	length of fixed bed
n	isotherm parameter
$\eta_1$	interaction coefficient
Q	isotherm parameter
$Q_{st,a}$	the apparent isosteric heat of adsorption
q	surface concentration
$q_e$	surface concentration at equilibrium
$q_s$	surface concentration at external surface

$\bar{q}$	reduced surface concentration ( $q/q_0$ )
$\bar{q}_0$	reduced surface concentration at external surface
$\bar{q}_s$	reduced surface concentration at partial surface
R	ideal gas constant ; adsorbent particle radius
r	internal radius of particle
$\bar{r}$	reduced radial distance, $r/R$
St	stanton number
T	temperature C or K
T'	throughput
t	time
V	total volume of solution
V <sub>p</sub>	volume of particle
v	interstitial velocity
v <sub>0</sub>	superficial velocity or flow rate
X <sub>m</sub>	amount of solute adsorbed in forming a monolayer
Z	axial coordinate of fixed bed
$\bar{Z}$	reduced axial distance, $Z/L_b$
$\rho$	particle density
$\phi$	sphericity



## CHAPTER 1.

### INTRODUCTION

#### 1-1 General Discussion

A vast quantity of organic compounds has been introduced recently to improve our living standards. Most of these compounds are the products from the procedure of synthesis by industries. The discharge of synthetic organic compounds into the environment will cause severe adverse effects including toxicity, carcinogenicity, taste and odor problems, and degradation of the quality of water for consumptive use. The potential impacts of hazardous organic pollutants in wastewater constitute a matter of steadily expanding concern for the water quality specialist. Control of toxic pollutants is also gaining increased emphasis in both water and wastewater treatment. Therefore, it is necessary to regulate the release of these organics to the environment and find methods to reduce or effectively remove these contaminants from water.

The Environmental Protection Agency (EPA) has developed a list of harmful chemicals. In the list, 129 pollutants are termed as priority pollutants. The reasons for singling out these priority pollutants are because of their : (1) frequencies of occurrence in water, (2) chemical stability, (3) quantities of the chemical produced, (4) availability of chemical analysis methods.

Phenol and its derivatives occupy a prominent position on the EPA priority pollutant list. In addition to being suspected carcinogens, phenol and some of its derivatives have been shown to be either toxic or lethal to fish at

concentrations of 5 to 25 mg/l (Khan, 1981). The presence of phenol at a concentration of only 2 mg/l imparts objectionable tastes and odors to drinking water when combined with chlorite, due to the formation of chlorophenols. In referring to the phenolic compounds, it is intended to include not only phenol itself but also chlorinated phenols. As a consequence, though p-chlorophenol (PCP) is not found in the EPA list of priority pollutants, it is of concern in this study due to the fact that it is a member of the chlorophenol family which was included in the list.

Phenol is recovered from coal tar, and large amounts are produced synthetically. It is used extensively in the synthesis of organic products, particularly in the production of phenolic type resins. Sources of phenolic compounds occurring as a natural compound in industrial wastes include effluents from coal-gas, coal-coking, and petroleum industries as well as in a wide variety of industrial wastes from processes involving the use of phenol as a raw material. Industries having the chlorophenol family in their wastewater are textile, ink metal finishing, steam electric, and leather tanning and finishing, etc.

Removal or reduction of these organic compounds to an acceptable level has become an increasing concern in the fields of water and wastewater treatment technology. Considerable efforts have been made by the EPA and other researchers to improve conventional techniques. The occurrence of maximum concentrations of phenol and p-chlorophenol in the raw wastewater and in treated industrial effluents are listed in Tables 1.1 and 1.2.

In the realm of dissolved organic contaminant control, treatment methodologies such as biological degradation, adsorption, ion exchange, chemical

oxidation, membrane separations, and incineration, have been applied. Adsorption on activated carbon has gained wide acceptance and is regarded as the most efficient and economical procedure for recovering undesirable materials from dilute aqueous solution. Activated carbon is obtained through a controlled oxidation process which results in a porous carbon structure with a large surface area. The large surface area gives the activated carbon a high capacity to adsorb organic materials.

Adsorption processes, especially those that use granular activated carbon, will find increasing use in wastewater and potable water treatment. It is necessary to know the adsorption capacity as well as the adsorption rate to design adsorption equipment. Adsorption capacity is usually expressed by an isotherm based on measured data. The rate of adsorption depends on both transport rate from the outer surface of the particles and also on the transport rate into the particles. One or both of these rates may determine the total rate of adsorption.

A breakthrough curve from the operation of carbon columns can be used to obtain the performance of activated carbon columns to remove specific organic pollutants and to determine the contact time required to produce the desired effluent concentration. Since operation of such columns is time consuming and expensive, several predictive mathematical models have been proposed to eliminate or greatly reduce the need for pilot studies. These models which are used for forecasting adsorption column require reaction coefficients for adsorption capacity and the adsorption rates. The former is obtained from batch equilibrium systems; and the latter is obtained from batch kinetic systems. These coefficients are determined from the aid of mathematical models.

Many researchers have been working on the phenomenon of activated carbon adsorption and have proposed many mathematical models in the literature. Almost all of them are based on the constant temperature assumption, while very few investigations incorporate the study of temperature effect and then only on a limited amount of data. It is noted that temperature might be changed abruptly or unexpectedly during operation under practical conditions. The main purpose of this research is to take into account the effects of variation of temperature on adsorption. The batch kinetic and fixed bed (column) studies were conducted with constant temperatures and compared with step change in temperature.

It will be helpful if a model incorporates temperature as a variable. A mathematical model developed to compare the performance of a fixed bed adsorber at constant temperature was modified to take into account influent temperature variations. Experiments were conducted to verify the predicted values from the modified mathematical model.

Table 1.1

Reported Maximum Concentrations for Phenol  
in Industrial Effluents

Industrial category	Max. Concentration Raw water ( $\mu\text{g}/\text{l}$ )	Reported Treated ( $\mu\text{g}/\text{l}$ )
Paint Formulating	3,800	1,240
Gum and Wood Chemicals	23,000	1,900
Leather Tanning	2,500	1,400
Ink Formulating	536	18
Textile Industry	4,900	50
Petroleum Refining	--	4,200
Pulp, Paper and Paperboard Industry	640	250
Coal Mining	3	--
Steam Electric Power Plant	100	--
Pulp and Paperboard Mills and Paper Coverts	624	89
Organic Chemicals Manufacturing	7,300	30
Pharmaceuticals	51,000	120

Source : EPA Development Document for Effluent Limitation Series

Table 1.2

Reported Maximum Concentrations for Chlorophenol  
in Industrial Effluents

Industrial category	Max. Concentration Raw water ( $\mu\text{g}/\text{l}$ )	Reported Treated ( $\mu\text{g}/\text{l}$ )
Paint Formulating	4,900	3,700
Gum and Wood Chemicals	47	--
Tiaber Product Processing	306	--
Ink Formulating	1,300	--
Textile Mills	940	15
Petroleum Refining	--	4,200
Pulp, Paper and Paperboard Industry	1,200	1,400
Lether Tanning and Finishing	6,200	1,700
Steam Electric Power Plant	12	4
Pulp and Paperboard Mills and Paper Coverts	--	--
Organic Chemicals Manufacturing	--	--
Paraceticals	62	--

Source : EPA Development Document for Effluent Limitation Series

## 1-2 Objectives and Scope of the Research

The objectives of the research are:

1. To establish adsorption isotherms for phenol and PCP at constant temperature and extend an available isotherm equation for various temperatures.
2. To assess the performance of an adsorption model to predict adsorption rates at constant temperature and step change in temperature from single and multicomponent systems.
3. To assess the ability of a fixed bed model to predict breakthrough curves at constant and step change in temperature from single component systems.
4. To compare the breakthrough curves for step changes in temperature for multicomponent systems.

The scopes of this research are as follows:

1. Establishment of adsorption equilibrium and kinetics of phenol and PCP.
  - (1) Single solute and multicomponent equilibrium studies were conducted to obtain isotherms at four different temperatures.
  - (2) Batch kinetic studies were conducted to determine adsorption rates and transport parameters. Adsorption rates were developed for single solute and multicomponent systems for constant temperature and for step changes in temperature.
2. Fixed bed (column) studies were conducted at two different temperatures. The experimental data from single component tests were used to compare

with prediction using a mathematical model. The goal was to show the validity of the model in predicting the breakthrough curves of fixed bed adsorption. For multicomponent tests, the results were applied to compare adsorption ability with different procedures of step change in temperatures.



## CHAPTER 2.

### REVIEW OF RELATED LITERATURE

#### 2-1 Single Solute Adsorption Models

##### 2-1-1 Equilibrium Models

Data collected during an equilibrium test will describe the performance of the activated carbon. Several mathematical relationships have been developed to describe the equilibrium distribution of solute between the solid and liquid phases. The equilibrium relationships defined as adsorption isotherms are plots between equilibrium concentration,  $C_e$ , which is the amount of organic compound left in solution, and surface concentration,  $q_e$ , the amount of compound on the surface of the activated carbon.

An adsorption isotherm equation usually represents equilibrium data at a given temperature. Three of the most common isotherm equations are the Langmuir isotherm, the Freundlich isotherm, and the Brunauer-Emmett-Teller (BET) isotherm. The Freundlich isotherm (Freundlich, 1926) which is basically empirical, is represented as

$$q_e = K C_e^{1/n} \quad (2.1)$$

or

$$\log q_e = \log K + 1/n \log C_e \quad (2.2)$$

A plot of  $\log q_e$  vs.  $\log C_e$  should yield a straight line for adsorption data which follow the Freundlich theory. The values of the constants  $K$  and  $n$  that must be evaluated for each solute and temperature are easily obtained from the straight line. Although the assumption was based on the fact that the adsorbent had a heterogeneous surface composed of different classes of adsorption

sites, the Freundlich isotherm is often useful as a means for data description. The Langmuir isotherm (Langmuir, 1918) is based on the assumption that the adsorbed layer will be monomolecular. The Langmuir isotherm is commonly written as

$$q_e = \frac{Q b C_e}{1 + b C_e} \quad (2.3)$$

In addition to the previous assumption, the Langmuir isotherm also assumes that energy of adsorption is uniform. Thus,  $Q$  is the number of moles of solute adsorbed by per unit mass of adsorbent in forming a complete monolayer on the adsorbent. The constant,  $b$ , is related to the energy of enthalpy of adsorption. Taking the reciprocal of both sides of Equation 2.3 yields two convenient linear forms of the Langmuir equation.

$$\frac{C_e}{q_e} = \frac{1}{Q b} + \frac{C_e}{Q} \quad (2.4)$$

or

$$\frac{1}{q_e} = \frac{1}{Q} + \frac{1}{Q b} \frac{1}{C_e} \quad (2.5)$$

A straight line will be obtained when the quantity  $1/q_e$  is plotted against  $1/C_e$ . Values of the constant,  $Q$  and  $b$ , can then be determined from the slope and intercept of the plot.

Neither the Freundlich nor Langmuir isotherms may describe the data satisfactorily over a wide range of concentration; therefore, an empirical equation with three parameters was applied by Redlich and Peterson (1959), Radke and Prausnitz (1972), and Mathews and Weber (1977) to describe adsorption isotherms when the concentration of the adsorbent varied widely.

$$q_e = \frac{A C_e}{1 + B C_e^A} \quad A \leq 1 \quad (2.6)$$

At low concentrations, this three parameter equation reduced to a linear form; while at high concentration, it becomes the Freundlich isotherm. For the special case of  $\beta = 1$ , it becomes the Langmuir isotherm. The parameters,  $A$ ,  $B$ , and  $\beta$  have to be determined by the best statistical representation of the experimental data. In this research, the three parameter equation is selected to describe equilibrium adsorption.

BET isotherm based on the assumption that molecules could be adsorbed more than one layer thick on the surface of the adsorbent. The equation is commonly written as

$$q_e = \frac{A C X_m}{(C_s - C) [ 1 + (A-1) C/C_s ]} \quad (2.7)$$

where  $q_e$  = amount of the solute adsorbed per unit mass of adsorbent

$C$  = concentration of the solute in solution at equilibrium

$C_s$  = saturation concentration of the solute

$X_m$  = amount of the solute adsorbed in forming a complete monolayer

$A$  = a constant to describe the energy of interaction between the  
the solute and the adsorbent surface

## 2-1-2 Batch Kinetic Models

The equilibrium distribution of solute between the liquid and solid phases is an important property of an adsorption system. Of equal importance to the engineer is the kinetics of the system which describe the rate at which equilibrium is reached. Process kinetics describing the rates at which molecules are transferred from solution to the surface of the carbon particles involve several sequential and parallel transport and reaction phenomena. Four distinct steps must take place for adsorption to occur:

- (1) The adsorbate solute passes through a film surrounding the adsorbent particle to the surface of the particle. (film transfer)
- (2) The adsorbed solute is transferred to an adsorption site on the inside of pore. (pore diffusion)
- (3) The adsorbed solute diffuses along the surface of the pore. (surface diffusion)
- (4) The solute becomes attached to the surface of the pore, i.e., is adsorbed. (adsorption)

Figure 2.1 represents the overall rates of adsorption of solute onto granular particles. Many factors influence the rates at which adsorption occur and the extent to which a particular material can be adsorbed. Several of the factors will be discussed in later sections.

There are many models which are commonly used for describing one or a combination of different rate processes. Different assumptions were made to simplify rate process by these models. Four of these models are :

A second-order reaction rate model was developed by Thomas (1949) for adsorption and ion-exchange reactions. Hiester and Verwey (1952) extended

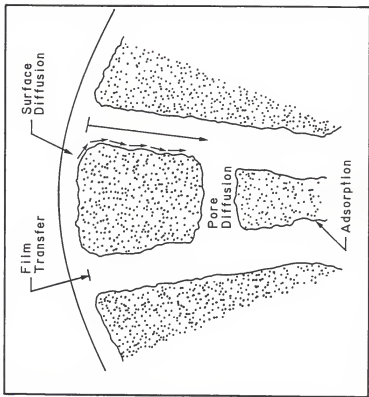


Figure 2.1 Adsorption on Porous Adsorbent  
Rate Limiting Mechanisms.

it to diffusion controlled adsorption. Keinath and Weber used this method to predict breakthrough curves for expanded fixed bed adsorption. In this method, the adsorption rate is equated to the diffusional rates to obtain the reaction rate constant in terms of the transport rate constant.

A second type of modeling approach is the application of linear driving force expressions for internal and external transport processes (Glueckauf, 1955; Wilde, 1980; Tien, 1981).

The pore phase diffusion model considers the adsorbent particles as consisting of a solid phase interspersed with very small pores. The adsorbate diffuses into the pores in the fluid phase, and adsorption occurs at the internal surface (Edeskuty and Amundson, 1952; Kesten, 1952; DiGiorno and Weber, 1969, 1972).

The homogeneous solid phase diffusion model proposed by Rosen (1952) will be outlined in detail. The model is developed for predicting adsorption rates in batch and fixed bed reactors. The model equations are solved numerically for three parameter isotherms with the film transfer and solid phase diffusion as the rate controlling steps. In a rapidly agitated batch reactor, the concentration of the solute  $C$  and the distribution of the adsorbent particle may be assumed to be uniform throughout the reactor. The film transfer from the fluid phase to the solid surface is expressed in terms of the time rate of change of the average solute concentration,  $q$ , of the particle. It can be shown as the following equation:

$$\frac{dq}{dt} = \frac{k_f A_p}{V_p \rho} (C - C_s) \quad (2.6)$$

where  $C$  is the concentration of the solute in the liquid expressed in

moles/liter;  $C_B$  is the equilibrium concentration in the liquid phase;  $k_f$  is the film transfer coefficient; and  $A_p$ ,  $V_p$ , and  $\rho$  are the surface area, volume, and density of the particle, respectively.

The average solute concentration of the entire particle with a radius of  $R(\text{cm})$  is obtained by integrating the pointwise concentration over the volume of the particles, thereby yielding

$$q = \frac{3}{R^3} \int_0^R q r^2 dr \quad (2.9)$$

For a spherical particle, assuming symmetry in two directions, transport within the solid phase is given by :

$$\frac{\partial q}{\partial t} = D_B \frac{\partial}{\partial r} \left( r^2 \frac{\partial q}{\partial r} \right) \quad (2.10)$$

or

$$\frac{\partial q}{\partial t} = D_B \left( \frac{\partial^2 q}{\partial r^2} + \frac{2}{r} \frac{\partial q}{\partial r} \right) \quad (2.11)$$

$q$  is the dimensionless solid phase concentration at an internal radius,  $r$ , and  $D_B$  is the solid phase diffusion coefficient. The mass balance for the batch reactor is

$$V \frac{dC}{dt} = -W \frac{dq}{dt} \quad (2.12)$$

$V$  is the volume of solution, and  $W$  is total weight of carbon. The initial and boundary conditions for the liquid and solid phases are given as

$$\text{at } t = 0 : C = C_0 \quad (2.13)$$

$$\text{at } t = 0, 0 \leq r \leq R : q = 0 \quad (2.14)$$

$$\text{at } t \geq 0, r = 0 : \partial q / \partial r = 0 \quad (2.15)$$

$$\textcircled{a} \quad t \geq 0, r = R :$$

$$\frac{R^2 k_f}{\rho} (C - C_S) = \frac{\partial}{\partial t} \int_0^R q r^2 dr \quad (2.16)$$

$$\textcircled{b} \quad r = R, C_S = f(q_S) \quad (2.17)$$

Equations 2.13 and 2.14 imply that the initial concentration of solute is  $C_0$  in the liquid phase and zero in the solid phase, respectively. Equation 2.15 implies that at any time greater than zero, the concentration gradient at the center of the particle is zero. Equation 2.16 gives the mass-balance on the adsorbent particles which can be obtained from substituting Equation 2.9 into Equation 2.8. Equation 2.17 is the isotherm relation between the surface and solution concentration of the solute. The three parameter equation, Equation 2.6, is used to describe equilibrium,  $q_S$ , at the external surface.



## 2-1-3 Fixed Bed Model

In deriving the fixed bed model the following assumptions are made.

- (1) Local equilibrium exists at the external surface of adsorbent particles.
- (2) Liquid diffusion resistance occurs at the external surface and can be described as film transfer.
- (3) An adsorbent particle is a homogeneous and spherically shaped solid.
- (4) The liquid phase is uniform across any bed section.
- (5) The effect of axial dispersion is negligible in the range of flowrate typical of a liquid adsorption system.
- (6) Diffusion coefficients and rate parameters are independent of concentration.

Equations incorporated in describing the fixed bed model include Equation 2.11 and Equations 2.13 to 2.17 as solid phase conditions. Other equations in the liquid phase conditions are given below:

$$\frac{\partial C}{\partial t} = -v \frac{\partial C}{\partial Z} - \left[ 3 \frac{1 - \epsilon_B}{\epsilon_B R} \right] k_f (C - C_s) \quad (2.18)$$

$$\text{at } t = 0, 0 \leq Z \leq L_b : C = 0 \quad (2.19)$$

$$\text{at } t \geq 0, Z = 0 : C = C_0 \quad (2.20)$$

Equation 2.18 gives the mass balance of the solute at any time in the bed. The rate of change in the concentration of solute is equal to the sum of the convective change in the concentration inside the bed and rate of mass transfer through the film to the solid surface. Here,  $v$  is the superficial liquid velocity,  $\epsilon_B$ , the porosity of bed, and  $Z$ , the bed depth. Equation 2.19 represents the initial condition to the bed at time zero. Equation 2.20 repr-

resents that at any time equal to and greater than zero, the solution concentration at the entrance to the bed is equal to the initial concentration.  $L_b$  is the length of bed, and  $C_0$  is initial solution concentration.

The above equations are transformed into non-dimensional form by introducing following variables:

$$\bar{r} = r / R$$

$$\bar{q} = q / q_e$$

$$\bar{q}_s = q_s / q_e$$

$$\bar{C} = C / C_0$$

$$\bar{C}_s = C_s / C_0$$

$$\bar{Z} = Z / L_b$$

$$\gamma = L_b / v$$

$$Dg = q_e (1 - \epsilon_B) / C_0$$

$$T' = t / \gamma Dg$$

$$E_d = D_s Dg \gamma / r^2$$

$$S_t = \kappa_f r (1 - \epsilon_B) / R$$

The non-dimensional fixed bed model then becomes :

$$\frac{\partial \bar{q}}{\partial T'} = \frac{E_d}{\bar{r}^2} \frac{\partial}{\partial \bar{r}} \left( \bar{r}^2 \frac{\partial \bar{q}}{\partial \bar{r}} \right) \quad (2.21)$$

$$\text{at } T' = 0, 0 < \bar{r} < 1 : \bar{q} = 0 \quad (2.22)$$

$$\text{at } T' > 0, \bar{r} = 0 : \partial \bar{q} / \partial \bar{r} = 0 \quad (2.23)$$

$$\text{at } T' > 0, \bar{r} = 1 :$$

$$S_T (\bar{C} - \bar{C}_s) = \frac{\partial}{\partial \bar{r}} \int \bar{q} \bar{r}^2 d\bar{r} \quad (2.24)$$

$$\text{at } \bar{r} = 1 : \bar{C}_s = f(\bar{q}_s)$$

$$\frac{\partial \bar{C}}{\partial T'} = - Dg \frac{\partial \bar{C}}{\partial \bar{Z}} - 3 Dg S_t (\bar{C} - \bar{C}_s) \quad (2.25)$$

$$\textcircled{*} \quad T' = 0, \quad 0 \leq \bar{Z} \leq 1 : \bar{C} = 0 \quad (2.26)$$

$$\textcircled{*} \quad T' > 0, \quad \bar{Z} = 0 : \bar{C} = f(T') \quad (2.27)$$

The differential equations in the fixed bed model have been successfully solved by the use of orthogonal collocation method (Liu and Weber, 1977; Crittenden et al., 1980). The collocation method presents one of the several other weighted residual methods. In this method, the unknown solution of a differential equation is approximated by a trial function having constants and/or functions. When the trial function is substituted into the differential equation, the residual is forced to zero at collocation points. The orthogonal collocation is a special case of the collocation method. The trial functions are a set of orthogonal polynomials and the collocation points are the roots of these polynomials. By the application of orthogonal collocation, the partial differential equations are reduced to first order ordinary differential equations.

## 2-2 Multicomponent Adsorption Models

### 2-2-1 Equilibrium Models

The most <sup>Simple</sup> simplest model for describing adsorption equilibrium in a multicomponent system is the Langmuir model for competitive adsorption (Butler and Ockrent, 1930, Markam and Benton, 1931). The basic assumptions of this model is the same as the Langmuir model for a single solute system. The equation is given as

$$q_i = \frac{Q_i b_i C_i}{1 + \sum b_j C_j} \quad (2.28)$$

The surface concentration of adsorbate  $i$ ,  $q_i$ , is expressed as a function of the solution concentration of all  $N$  adsorbates in the mixture. The parameter,  $Q_i$ ,  $b_i$ , are obtained directly from single solute system.

The Langmuir competitive equation has been modified by Schay et al. (1985) by the use of interaction terms to improve the description of equilibrium data. The model is represented as

$$q_i = \frac{Q_i b_i (C_i/\eta_i)}{1 + \sum b_i (C_i/\eta_i)} \quad (2.29)$$

where  $\eta_i$  is the interaction term for each solute, this term is evaluated by correcting the model to multicomponent experimental data. The main reason of introducing interaction terms is that interaction between components in a mixture can reduce the adsorption of some components to levels below that predicted from the single solute isotherms.

Mathews (1975) has extended the three parameter isotherms to multicomponent adsorption which is expressed as

$$q_i = \frac{A_i C_i}{1 + \sum B_j C_j^{A_j}} \quad (2.30)$$

The values of  $A_i$ ,  $B_i$ , and  $A_i$  are obtained from single solute systems that are described by the three parameter isotherm. Also, Mathews has proposed the use of an interaction term, as done by Schay et al. (1975), to adequately describe a multicomponent system. As a result, Equation 2.30 is then given as

$$q_i = \frac{A_i (C_i/\gamma_i)}{1 + \sum B_j (C_j/\gamma_j)^{A_j}} \quad (2.31)$$

The interaction coefficients,  $\gamma_i$ , are calculated by the correlation of mixture equilibrium data.

The ideal adsorbed solution model (IAS model) has been developed from dilute solution thermodynamics by Redke and Prausnitz (1972a) using the method of Myers and Prausnitz (1965) for gas mixtures. The model predicts multicomponent equilibrium by using single solute isotherms. The basic assumptions of the IAS models are:

- (1) The available specific surface area is identical for all adsorbates.
- (2) The adsorbent is thermodynamically inert.
- (3) Single solute isotherm data are required to extremely low concentrations, generally below  $5 \times 10^{-5}M$  and varying with the solutes.
- (4) The adsorbed phase forms an ideal solution.

For strongly adsorbed solutes, predicted results are not in good agreement with experimental data.

### 2-2-2 Batch Kinetic Models

Weber and Morris (1964), in their studies on competitive adsorption from solution containing two solutes, found that each solute adversely affected the rate of adsorption in the presence of the other solute. But, the overall rate of adsorption was greater than those for either of the individual substances from its pure solution.

Tien and Thodos (1976) described ion-exchange kinetics using the homogeneous solid phase diffusion and a Freundlich type isotherm. Brecher et al. (1973) provided finite difference approximations for the model using BET isotherm. Finite difference approximations were developed for any arbitrary isotherm by Mathews and Weber (1975). They also extended the model to multi-component systems and verified the model for batch adsorption for a wide range of binary mixtures. This approach has been successfully applied to several solutes and mixtures in batch reactors and fixed beds (Crittenden and Weber, 1978; Lee et al. 1980; Weber and Liu, 1980; Weber and Pirbazeri, 1981; Thacker et al, 1981).

### 2-2-3 Fixed Bed Models

Yen and Singer (1984) applied the IAS model with a modified calculation to test ten sets of binary and tertiary phenolic mixtures. The Langmuir competitive model was used for comparison. The IAS model was found to be successful in precisely describing the competitive adsorption equilibria of phenolic mixture and was proven to be superior to the Langmuir competitive model in all cases of studies.

Crittenden and Weber (1978a, 1978b, 1978c) have studied single solute and bisolute adsorption of the same solutes and adsorbent as used by Mathews (1975). They used the homogeneous solid diffusion model as a basis. The film transfer and the solid phase diffusion coefficients were calculated from single solute batch kinetic experiments as mentioned in the last section. The model successfully described the single solute fixed bed but not from multicomponent fixed bed experiments. The discrepancies observed were thought to be due to (1) experimental data scatter; (2) poor equilibrium description; (3) failure of the assumption of independent diffusion of solute.

## 2-3 Factors Influencing Adsorption

### 2-3-1 Temperature

The temperature at which an adsorption process is conducted will affect both the rate of adsorption and the extent to which adsorption occurs. Adsorption rate parameters generally increase with increased temperature and decrease with decreased temperature. The extent of adsorption will increase with a decrease in the lower temperature and decrease with an increase in the higher temperature due to being an exothermic nature of the adsorption reaction.

Because water is adsorbed from the surface when adsorption from aqueous solution occurs, heat effects for the process are somewhat smaller in comparison with gas-phase adsorption. Heat of gas-phase adsorption generally is several Kcal per mole. Thus small variations in temperatures do not tend to alter the adsorption process to a significant extent for solid phase adsorption.

Suzuki and Kawazoe (1975) studied adsorption of fifteen kinds of volatile organics on activated carbon from aqueous solution carried out in a batch system. They assumed that the adsorption rate was controlled by intraparticle diffusion and the solid phase diffusion coefficients for each organic was determined by applying the concentration-time curves. The solid phase diffusion coefficient,  $D_s$  ( $\text{cm}^2/\text{sec}$ ), thus obtained, is successfully correlated to the ratio of the boiling point of adsorbate and to adsorption temperature as

$$D_s = a \exp \left( -b \frac{T_b}{T} \right) \quad (2.32)$$



where a and b are constants from experimental data.

Sudo and Suzuki (1978) determined the concentration dependence of the solid phase diffusion coefficient during adsorption from the aqueous phase. The solid phase diffusion coefficient,  $D_s$ , was determined as a function of the amount of solute adsorbed on the carbon,  $q$ . Based on the data obtained, it follows that  $D_s$  increased with  $q$  and that  $\log D_s$  vs  $q$  has a constant slope for all organics investigated within the range of the amount adsorbed. The following relationship represented the result.

$$D_s = D_{s0} \exp(a q) \quad (2.33)$$

where  $D_{s0}$  was determined from  $D_s$  values extrapolated to where  $q = 0$ .

Suzuki and Fujii (1982) studied concentration dependence of surface diffusion coefficients of propionic acid in activated particles. They conducted a separate set of experiments from which adsorption relations were determined by batch adsorption at 283°K, 293°K, 303°K, 313°K for a wide range of concentration from  $2 \times 10^{-3}$  to 20 mole/m<sup>3</sup>. Strong dependence of  $D_s$  on  $q$  is partially interpreted in terms of the change of heat of adsorption with surface coverage as determined from separate equilibrium runs. The  $D_s$  values were calculated by a steady state technique for determining dependence of the  $D_s$  on amount of adsorption which was proved to be useful. The steady state diffusion experiment was performed with varying concentrations of propionic acid solution passed through activated carbon pellets. The following equation represents the relation between  $D_s$ ,  $T$  and  $q$ .

$$D_s = D_{s0} \exp \left[ - \frac{Q_0}{R T} \ln(a q) \right] \quad (2.34)$$

$Q_0$  is obtained from the following equation.

$$Q_{st,a} = - Q_0 \ln(a q) \quad (2.35)$$

where  $Q_{st,a}$  is isosteric heat of adsorption. It can be defined as

$$Q_{st,a} = R \frac{d \ln C}{d (1/T)} \quad (2.36)$$

## 2-3-2 Other factors

### Surface Area

Adsorption is a surface phenomenon as such, the extent of adsorption is proportional to specific surface area. The definition of specific surface area is the portion of surface area that is available for adsorption. Thus the amount of adsorption accomplished per unit weight of a solid adsorbent is greater the more finely divided and the more porous solid.

### Agitation

The rate of adsorption is controlled by either film transfer or surface diffusion, depending upon the intensity of agitation in the system. If relatively little agitation occurs, the film transfer will likely be the rate-limiting step because of the surface film around the particle will be thick. For a continuous-flow system of flowrate less than 10 gal/ft<sup>2</sup>-min, the film transfer will be rate-limiting. If adequate mixing is provided like in batch-type contacting system, surface diffusion is generally rate limiting.

### Size of Carbon Particles

Morris and Weber (1964,1964a) reported that the rate of adsorption correlated with the inverse of the square of the diameter of carbon particles. Specifically, adsorption rates increase with as particle sizes decrease. They also observed a significant increase in adsorption capacity with decrease in carbon particle size.

In the column system, the time required to reach the breakpoint increased linearly with decrease in particle size. After the breakpoint, however, the approach to the exhaustion capacity of the carbon column speeded up with decreasing particle size (Martin 1978).

### Solubility of Adsorbates

In general, an inverse relationship can be anticipated between the extent of adsorption of a solute and its solubility in the solvent from which adsorption occurs. The greater the solubility, the stronger the solute-solvent bond and the smaller the extent of adsorption.

### pH

Adsorption of typical organic pollutants from water is increased with decreasing pH. In many cases this may result from neutralization of negative charge at the surface of the carbon with increasing hydrogen-ion concentration, thereby, reducing hindrance to diffusion and making available more of the activated surface of the carbon.

## CHAPTER 3.

### EXPERIMENTAL MATERIALS AND METHODS

#### 3-1 Materials

##### 3-1-1 Adsorbents

The adsorbent used in this research was granular activated carbon. The physical properties of the carbon are listed in Table 3.1.

Filtrisorb-400 were chosen for all experiments in this study. The carbon is received as 12/40 (particles passing through a U.S. Standard Mesh Size No.12 screen but retained on No.40 screen) and is sieved to 20/25 to give a narrower size range for batch kinetic and fixed bed studies. The geometric mean diameter of a particle is given by  $(d_1 d_2)^{1/2}$  where  $d_1$  is the mesh size of upper sieve and  $d_2$  is the mesh size of the lower sieve. Based on this, particles passing through U.S. mesh size No.20 and retained on U.S. mesh size No.25 had a diameter of 772 microns. For equilibrium studies, some carbon particles were ground to provide a small particle size 200/230. Before experiments, the carbon was washed several times in distilled deionized water, dried to constant weight in an oven at a temperature of 103°C and kept at room temperature in airtight containers pending use.

Table 3.1

## Properties of Activated Carbon

---

Manufacturer	Calgon Co. PA
U.S. Mesh Size	20 / 25
Raw Material	Bituminous Coal
Physical Properties	
surface area, $m^2/gm$	1000 - 1100
apparent density, $gm/cc$	2.1
particle density, $gm/cc$ wetted in water	1.35
effective size, $mm$	0.71 - 0.84
uniformity coefficient	1.9 or less
backwashed and drained density, $lb/ft^3$	25

---

### 3-1-2 Adsorbates : Phenol and Parachlorophenol (PCP)

The adsorbates used in this research were phenol and parachlorophenol (PCP) with their properties listed in Table 3.2. Both adsorbates were supplied by J.T. Baker Chemical Co. in crystal form stored in dark glass bottles.

All stock solutions were prepared with organic-free distilled water. The system to obtain this water was a 4-stage filter which is able to remove organic compounds in tap water and produce ultra pure distilled water. The stock solutions were stored in a freezer and diluted to the desired concentration prior to use. The pH values through experiments were kept constant at 7.

Table 3.2

## Adsorbates and Their Properties

	Phenol	PCP
Supplier	J.T. Baker Commercial Co.	J.T. Baker Commercial Co.
Grade	Baker Reagent Grade	Baker TM
Formula	$C_6H_5OH$	$C_6H_4OHCl$
M.W.	94.1	128.58
pKa	9.90	9.18
Melting point	43°C	42-44°C
Boiling point	181.75°C	-
Diffusivity in water ( $10^{-6}$ cm <sup>2</sup> /sec)	9.12 at 20°C 10.43 at 25°C 11.83 at 30°C 13.33 at 35°C	8.71 at 20°C 9.96 at 25°C 11.32 at 30°C 12.74 at 35°C



## 3-2 Methods

### 3-2-1 Analytical Methods

The concentrations of phenol and PCP solutions were analyzed by ultraviolet absorption spectrophotometry using a Bausch & Lomb Spectronic 710 Spectrometer. The wavelengths of maximum absorbance for phenol and PCP were determined in preliminary tests. Several standard solutions of phenol and PCP were prepared after the wavelengths of maximum absorbance were measured. To obtain significant absorbance when analyzing low concentration samples, 50 mm photocells were used, whereas more concentrated samples were analyzed with a 10 mm photocell. Calibration curves of standard solutions were determined for light path lengths of 10 mm and 50 mm.

Phenol was analyzed at a wavelength of 268 nm and PCP at 279 nm. Table 3.3 shows the selected wavelengths and the corresponding molar absorptivities which are determined from the slopes of the calibration curves.

Mixtures of phenol and PCP were analyzed at wavelengths of 268 nm and 279 nm. The procedure developed by Friedel (1951) was employed to compute individual concentrations of phenol and PCP. Note that underlying assumption of the Friedel's procedure is that the absorbance of a mixture can be expressed as a linear combination of that of its compounds at a given wavelength. As a result, the following set of simultaneous equations are used to determine the concentration of phenol and PCP in a mixed system.

$$A_{268} = \epsilon_{P1} C_P + \epsilon_{PCP1} C_{PCP} \quad (3.1)$$

$$A_{279} = \epsilon_{P2} C_P + \epsilon_{PCP2} C_{PCP} \quad (3.2)$$

where

$A_{268}, A_{279}$  = the absorbance of the mixed solution at wavelengths of 268, 279 nm, respectively.

$C_p, C_{PCP}$  = concentration of phenol and PCP, respectively.

$\epsilon_{p1}, \epsilon_{PCP1}$  = Molar absorptivities of phenol and PCP at a wavelength of 268 nm.

$\epsilon_{p2}, \epsilon_{PCP2}$  = Molar absorptivities of phenol and PCP at a wavelength of 279 nm.

The concentrations of Phenol and PCP, i.e.,  $C_p$  and  $C_{PCP}$ , respectively, can be determined by solving the above simultaneous equations.

Table 3.3

Molar Absorptivities of Adsorbates (l/mole-cm)

wavelength (nm)	phenol	PCP
268	1463	887
279	592	1438

### 3-2-2 Equilibrium Experiments

Equilibrium experiments were carried out by the standard bottle-point method. Different amounts of particles (200/230) were weighed carefully and put into a series of 125 ml glass bottles which contained 100 ml of phenol and/or PCP solution with concentration. Carbon was prepared by washing samples several times with deionized water to remove fines. Glass bottles were washed thoroughly and dried in an oven at 103°C. Carbon dosages varying from 0.1 - 2.2 gm were added to the bottles prepared earlier as a adsorbate. The bottles were sealed with caps to ensure airtight and placed in a Controlled Environment Incubator Shaker (Labline Instruments Inc., Ill) to provide agitation at desired temperatures.

In each experimental run, the initial solute concentration,  $C_0$ , was recorded at the outset of the run, followed by measurement of the bulk solute concentration,  $C_e$ , on a daily basis; the amount of solute adsorbed per unit mass of activated carbon,  $q_e$ , was thus determined as

$$q_e = \frac{C_0 - C_e}{W} V \quad (3.3)$$

where  $W$  is the total weight of the carbon, and  $V$  is the volume of solution. It is worthwhile mentioning here that measurement of solute concentration involved a two-step process. In step one, the samples were filtered through a 23  $\mu$ m membrane filter (Gelman Science Co.) to remove any suspended carbon; the solute (filtrate) concentration was then measured subsequently. The amount of each solute adsorbed on the carbon at equilibrium was calculated from the mass-balance Equation 3.3. Each bottle represents one point on the equilibrium curve. By using different initial concentrations and by varying the

carbon dosage, the isotherm profile can be determined. The isotherm data are plotted typically on log-log paper. The concentration remaining in solution after equilibrium,  $C_e$ , are plotted on the abscissa ; the amount of solute adsorbed per unit weight of activated carbon,  $q_e$ , are plotted on the ordinate. The resulting plots represent the adsorption isotherms. A series of adsorption isotherm data were then determined.

To provide an environment with constant temperature for equilibrium experiments, the Controlled Environment Incubator Shaker was set to a desired temperature. The shaker was adjusted so that the adsorbent was always kept suspended, care being taken to see that the adsorbent did not stick to the sides of the bottles. Before filtration, the bottles were removed from the shaker, and they were partially immersed in a bath in which the temperature was maintained at the same temperature as that of the Environment Incubator Shaker.

Four different temperatures, 20°, 25°, 30°, and 35°C, were tested for experiments with single solute. In cases of mixtures, the experiments were conducted under only two temperatures, namely, 20° and 35°C.

### 3-2-3 Batch Kinetic Experiments

Carbon adsorption processes investigated in this study were operated on both batch and fixed bed basis. The former is discussed in this section while the latter will be elaborated in next section.

Batch experiments were conducted to evaluate the film transfer coefficient ( $k_f$ ) and the solid phase diffusion coefficient ( $D_s$ ) on carbon of phenol and PCP at various temperatures. Batch kinetic experiments were conducted in a rectangular vessel made of plexiglass. The dimensions of the vessel were 34 cm x 30 cm x 36 cm which are L, B, and H, respectively. Wall thickness was 0.68 cm. A steel impeller was located at the center of the vessel and 7 cm from the bottom. A 1000 watt heater and a temperature-controller were used to regulate the temperature of the solution. The schematic of experimental facilities are illustrated in Figure 3.1. The rate experiments were normally conducted for a duration of 3 or 3.5 hours.

A solution of 24 liters was prepared from tap water passed through a three carbon columns to remove suspended and organic matter. The depth of each solution from the bottom was about 23.5 cm. In no experiments were crystals of solute directly introduced into the vessel. In all cases, stock solutions with the desired concentration were made up. The impeller was maintained at a speed of 700 rpm to agitate the solution to reach equilibrium within the vessel. A fixed amount of solution was withdrawn to determine the initial concentration after the impeller ran steadily. A predetermined amount of carbon was poured abruptly into the reaction vessel at which moment the time started counting. Samples were withdrawn from the vessel with a pipet to analyze concentration at selected time intervals.

The size of carbon particle used in experiments ranged from U.S. mesh size No.20 to No.25. The total weight of the carbon used was 6 gm. The solution was preheated, if necessary, to the desired temperature. A temperature controller was used to keep the temperature at a constant value. For a step change in temperature, solution was held constant in the first hour followed by the use of a heater or dry ice for an increase or decrease in temperature. It took 15 minutes to raise the temperature from 20°C to 35°C. To decrease temperature, approximate 1.5 lb of dry ice was introduced into the vessel, and it took 20 minutes to bring down the temperature from 35° to 20°C. For constant temperatures, four runs, each with temperature of 20°, 25°, 30°, and 35°C, respectively, were carried out for single solute studies; two runs, each with temperature of 20° and 35°C, respectively, were for mixture. For step changes, two runs were done. One with the temperature increased from 20° to 35°C and the other with temperature decreased from 35° to 20°C.

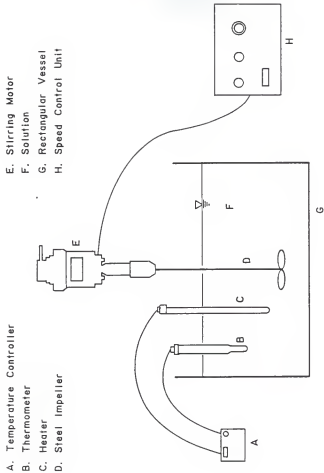


Figure 3.1 Schematic of Batch Kinetic System.



### 3-2-4 Fixed Bed Experiments

Figure 3.2 depicts the schematic of the fixed bed experiment. The fixed bed was a plexiglass tube with an inner diameter of 3.1 cm and a height of 6 feet. Glass beads with 2 mm diameter were filled at the bottom of the column as a velocity distributor and maintained uniform upflow velocity. Its function was to distribute the solution if the fixed bed employed upflow of liquid. In the research, all experiments were conducted with downflow. A 140-mesh brass screen separated the carbon in the column from the glass beads in the velocity distributor. A 30-gallon tank supplied a continuous flow of water to the top of the column as downflow of solution; the water was produced by having tap water run through a three-foot long filter filled with activated carbon to remove organics and other adsorbates from water. Two variable flow pumps were manipulated to force the water as well as the concentrated solution at a combined constant flowrate of 125 ml/min. The solution stored in a solution jar was prepared at a higher concentration than that was required. Simultaneous adjustments on the flows of the concentrated solution, and distilled water were performed to obtain a desired influent solution concentration. Constant checks on this influent concentration were required to ensure a minima variation in flowrate. The fixed bed experiments were generally conducted until the ratio of effluent concentration to influent concentration reached 0.95. The durations of the experiment were usually from 10 to 15 hours.

The desired influent solution temperature was obtained by mixing the concentrated solution at an ambient temperature with the pre-adsorbed tap water at a higher temperature; the determination of the distilled water temperature involved trial-and-error efforts. As an example, distilled water

was preheated to a temperature of 54°C so as to produce a resultant solution with a desired temperature of 35°C. Prior to the experiment the bed was fluidized for 30 minutes to remove trapped bubbles in the activated carbon zone.

For constant temperature studies, temperatures were selected at 20° and 35°C for runs with single solution. For step change in temperature studies, the temperature was held constant for the first three hours of the experiment before the step change. It took 30 minutes to raise the temperature from 20° to 35° and 25 minutes to reduce the temperature from 35°C to 20°C. Temperature settings were the same as those described in the kinetic experiment section.

Effluent solutions were collected and analyzed for determination of concentration. Breakthrough curves were hence obtained by plotting the ratio of effluent to influent concentration,  $C_i/C_o$ , versus time,  $T$ .

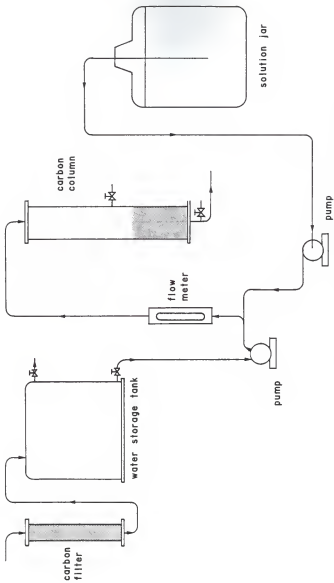


Figure 3.2 Schematic of Fixed Bed Adsorption System .

## CHAPTER 4.

### SINGLE SOLUTE ADSORPTION

#### 4-1 Equilibrium Studies

The three parameter equation, which reduces to the linear, or Langmuir isotherm, was employed to correlate the equilibrium relationship between the surface concentration,  $q_e$ , and the bulk solution concentration,  $C_e$ . The equation mentioned in Section 2-1 is

$$q_e = \frac{A \times C_e}{1 + B \times C_e^g} \quad (2.6)$$

The parameters, A, B, and g, which were determined by the best statistical representation of the experimental data, could be estimated by a nonlinear parameter estimation technique developed by Mathews (1975).

Experimental results of  $q_e$  and  $C_e$  obtained in Section 3-2-2 were fitted by Equation 2.6 with parameter values summarized in Table 4.1 at the four temperatures, 20°, 25°, 30°, and 35°C. The corresponding data are plotted in Figures 4.1 through 4.8. In these figures, it is observed that the extent of adsorption increases with a decrease in the temperature; this phenomenon conforms the well-known fact that adsorption is an exothermic process in general.

Since the three parameter equation is suitable only for a fixed temperature, its applications are of limited use in practice. As a remedy, an attempt was made to find the temperature dependencies of A, B, and g, in Equation 4.1. The method is similar to that proposed by Danner (1983). The five parameters,  $Q_0$ ,  $B_0$ ,  $g_0$ , K1, and K2 were evaluated by running a program

with entire equilibrium experimental data. By many trial steps, Equation 4.1 was found having the closest correlation.

$$q_e = \frac{Q_0 \exp(K1/T) C_e}{1 + B_0 \exp(K2/T) C_e^{\beta}} \quad (4.1)$$

It is apparent that A, B, and  $\beta$  can be represented by Equation 4.2 through 4.4 by applying T and the five parameters as variables.

$$A = Q_0 \exp(K1/T) \quad (4.2)$$

$$B = B_0 \exp(K2/T) \quad (4.3)$$

$$\beta = \beta_0 \quad (4.4)$$

The resultant parameter values of  $Q_0$ ,  $B_0$ ,  $\beta_0$ , K1, and K2 are listed in Table 4.2. Table 4.3 contains the values of A, B, and  $\beta$  calculated from Equations 4.2 to 4.4. Note that in the parameter estimation,  $\beta$  is maintained temperature independent.

In Section 2-3-1, the isosteric heat of adsorption,  $Q_{st,a}$ , can be calculated from Equation 2.36.

$$Q_{st,a} = R \frac{d \ln C}{d (1/T)} \quad (2.36)$$

The plots of  $\ln C$  versus  $1/T$  for  $q = 0.2, 0.4, 0.6, 0.8,$  and  $1.0$  mole/gm are showed in Figure 4.9. From the slopes, the values of  $Q_{st,a}$  were determined.

Figure 4.10 illustrated  $Q_{st,a}$  as a function of  $q$ . From the experimental results, the relationship can be represented by Equations 4.5 and 4.6.

phenol:

$$Q_{st,a} = -10625 \times \ln(0.167 q) \quad (4.5)$$

PCP:

$$Q_{st,a} = -15845 \times \ln(0.331 q) \quad (4.6)$$

Table 4.1

## Isotherm Parameters for Phenol and PCP

adsorbate	temp(°C)	A	B	$\beta$
phenol	20	36.37	20.34	0.7705
	25	32.53	19.26	0.7995
	30	27.09	17.64	0.8069
	35	22.50	15.43	0.8272
PCP	20	42.23	24.72	0.8791
	25	39.56	26.89	0.8654
	30	15.78	28.65	0.8747
	35	33.16	29.32	0.8503

unit of Equilibrium conc. as mmole/l

unit of surface conc. as mmole/gm

Table 4.2

Adsorption Equilibrium Constants for  
a Range of Temperature

Constants	phenol	PCP
Q <sub>o</sub>	0.1515	1.1090
B <sub>o</sub>	15.20	25.12
$\rho$	0.7838	0.8500
K <sub>1</sub>	1595.	1057.
K <sub>2</sub>	63.32	22.31

Table 4.3

## Isotherm Parameters for Phenol and PCP

Calculated from Equations 4.2 through 4.4

adsorbate	temp(°C)	A	B	$\beta$
phenol	20	35.04	18.87	0.7838
	25	31.98	18.80	0.7838
	30	29.28	18.73	0.7838
	35	26.88	18.67	0.7838
PCP	20	40.89	27.11	0.8500
	25	38.49	27.07	0.8500
	30	36.30	27.04	0.8500
	35	34.30	27.00	0.8500

unit of Equilibrium conc. as mole/l

unit of Surface conc. as mole/gm



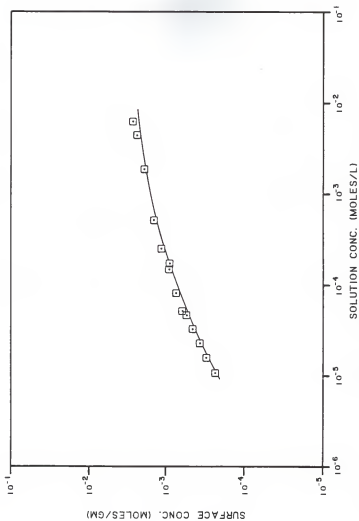


Figure 4.1 Adsorption Isotherm for Phenol at 20°C.  
(  $\square$  ) exp , ——— model)

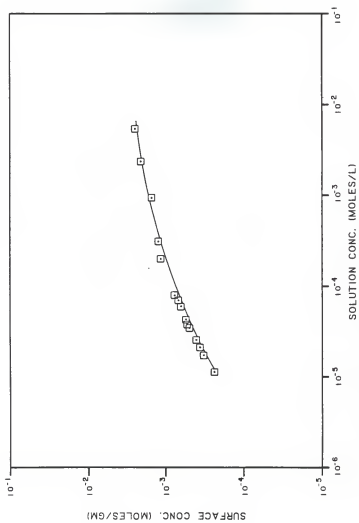


Figure 4.2 Adsorption Isotherm for Phenol at 25°C.  
(  $\square$  exp , — model)

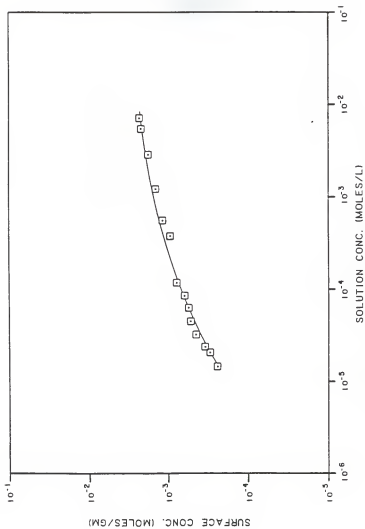
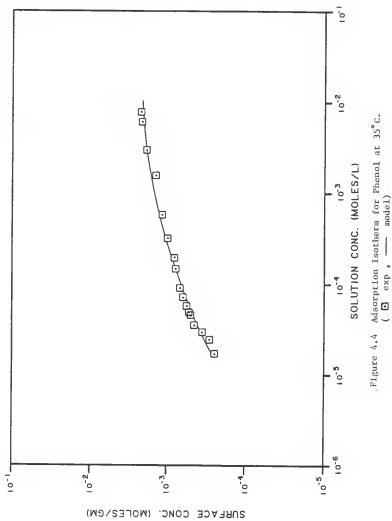


Figure 4.3 Adsorption Isotherm for Phenol at 30°C.  
(  $\square$  exp, — model)



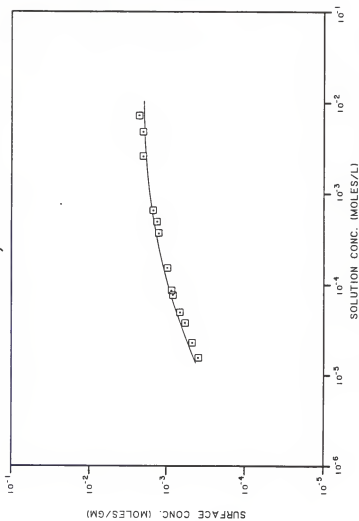


Figure 4.5 Adsorption Isotherm for PCP at 20°C.  
(□ exp, — model)

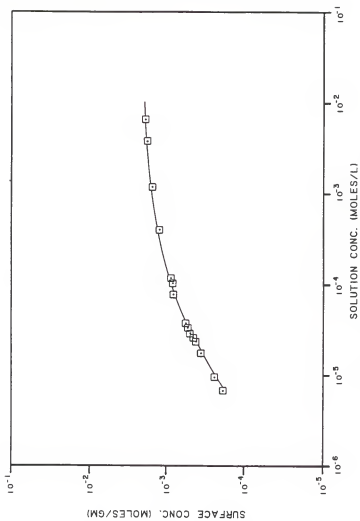


Figure 4.6 Adsorption Isotherm for PCP at 25°C.  
(  $\square$  exp, — model)

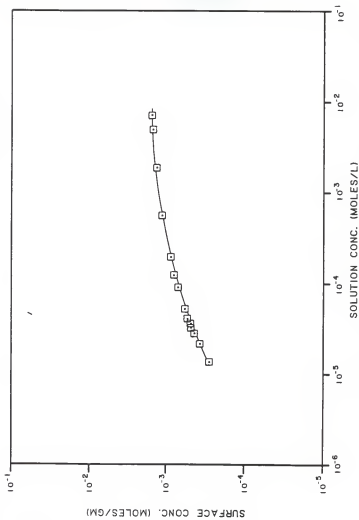


Figure 4,7 Adsorption Isotherm for PCP at 30°C.  
(  $\square$  exp , — model)

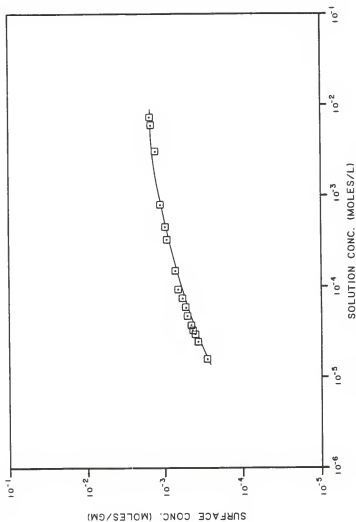


Figure 4.8 Adsorption Isotherm for PCP at 35°C.  
(  $\square$  exp, — model)



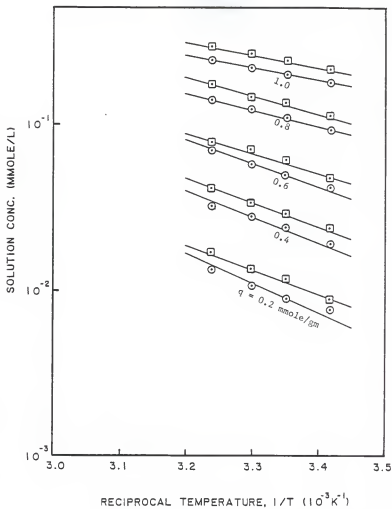


Figure 4.9 Adsorption Isotherms for Determining  
Isosteric Heat of Adsorption  
(  $\square$  Phenol ,  $\circ$  PCP )

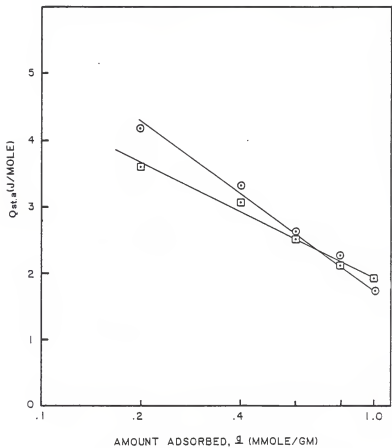


Figure 4.10 Isosteric Heat of Adsorption  $Q_{st,a}$  plotted against Amount Adsorbed  $q$  ( $\square$  Phenol,  $\circ$  PCP)

## 4-2 Batch Kinetic Studies

The objectives of batch kinetic studies were to determine the solid phase diffusion coefficients,  $D_s$ , and the film transfer coefficients,  $k_f$ , of phenol and PCP. Carbon size of 20/25, stirring speed of 700 rpm, reaction volume of 24 liters and total carbon weight of 6 gm were used in all batch kinetic experiments. The initial concentration of phenol and PCP was  $2.5 \times 10^{-4}$  M. The pH values were kept at 7. The reason for keeping the pH values at 7 is that the solution will contain almost 100% of phenol. The  $pK_a$  value of phenol is 9.9. If the pH value greatly less than  $pK_a$ , the concentration of  $C_6H_5O^-$  approach zero.

The homogeneous solid phase diffusion model proposed by Rosen (1952) was provided to predict the adsorption rates in batch reactors. The principal parameters required for use of the model are the film transfer coefficient,  $k_f$ , the solid phase diffusion coefficient,  $D_s$ , and the isotherm parameters. The film transfer coefficients,  $k_f$ , were determined by using the phenol or PCP concentration data obtained during the initial concentration. Equation 4.7 shows the calculation of  $k_f$ .

$$k_f = \frac{-\ln(C/C_0)}{t} \frac{(1 - \epsilon) \rho}{3 W / V} \frac{R}{2} \quad (4.7)$$

The values of  $\ln(C/C_0)$ ,  $C$  as adsorbate concentration at time  $t$ , and  $C_0$  as initial concentration, were plotted versus time  $t$ . The linear portion of time points were fitted with a straight line. The values of  $k_f$ , thus, were calculated from the slope. At longer contact time, the line become nonlinear because of increasing influence of intraparticle resistance.

A parameter estimation procedure used in the homogeneous solid phase model

was demonstrated to provide accurate estimates of the values of  $k_f$  and  $D_s$ . Intraparticle diffusion coefficients of the components were estimated by matching the predictions of the model to the results of batch kinetic experiments. A computer program written by Mathews (1975) was used to estimate  $k_f$  and  $D_s$  from batch reactor data. The input data of the program include isotherm parameters, the volume of solution, total weight of carbon, diameter of particle, initial concentration of solution, and initial estimates for  $D_s$  and  $k_f$ . This program uses the principal axis (Brent 1971) for finding the minimum of a function, and search for parameter values or  $k_f$  and  $D_s$  that will minimize the sum of the square of the difference between experimental and computed values of adsorption rates.

Figures 4.11 through 4.14 show the results for constant temperature experiments. In these figures the solid lines represent the best fit of the batch reactor model to the experimental data. The values of the film transfer coefficient,  $k_f$ , and the solid phase diffusion coefficient,  $D_s$ , are listed in Table 4.4. Comparison of the curves shows that PCP has higher adsorption rates than those of phenol. From experimental results, both the film transfer and solid phase diffusion coefficients increase with increasing temperature.

For step change experiments, two tests were run for phenol and PCP, that is, from 20° to 35°C and from 35° to 20°C. The computer program originally could only predict the coefficients at constant temperatures. A modification developed by Mathews (1984) takes into account temperature as a variable in fitting step change experiments. In the modification, Equation 2.6 was first substituted by Equation 2.1 to include temperature effect on the adsorption capacity. The film transfer coefficient,  $k_f$ , and the solid phase diffusion coefficient,  $D_s$ , following the Arrhenius' Law, were represented as

Equation 4.8 through 4.11.

$$\text{phenol: } k_f = 3.58 \times e^{-1975.3/T} \quad (4.8)$$

$$D_s = 6.4637 \times 10^{14} \times e^{-15437/T} \quad (4.9)$$

$$\text{PCP: } k_f = 71.144 \times e^{-2863.3/T} \quad (4.10)$$

$$D_s = 1.857 \times 10^6 \times e^{-9473.3/T} \quad (4.11)$$

where T represents the absolute temperature  $^{\circ}\text{K}$ . The above equations result from least-square fitting of the data in Table 4.6. The values calculated from the equations above are listed in Table 4.7. The plots of  $-\ln(k_f)$  and  $-\ln(D_s)$  versus  $1/T$  are shown in Figure 4.15.

It was mentioned that 15 minutes was needed to raise the temperature from  $20^{\circ}\text{C}$  to  $35^{\circ}\text{C}$  for the batch kinetic experiments. In predicting the adsorption rates for step changes, the program must consider the time required for the step changes in temperature. After the first hour of constant temperature operation, the temperature was assumed to be  $25^{\circ}\text{C}$  from 60 to 68 minutes,  $30^{\circ}\text{C}$  from 68 to 75 minutes and  $35^{\circ}\text{C}$  thereafter. Consequently, during each temperature range, the isotherm parameters,  $k_f$  and  $D_s$ , corresponding to that temperature were used.

Figures 4.16 and 4.17 show the experimental data and predicted curves for the step change in temperature of phenol and PCP. For the runs from  $20^{\circ}\text{C}$  to  $35^{\circ}\text{C}$ , the experimental data are in good agreement with the predicted curves. For the runs from  $35^{\circ}\text{C}$  to  $20^{\circ}\text{C}$ , the experimental data gives a fair fit with the predicted curves. This could be due to the changes of adsorption rates and stirring speed during the sublimation when putting dry ice in the solution to decrease the temperature. The two curves in Figure 4.14 and 4.15 have intersections. The intersections are based on that adsorption rates changed

abruptly during the temperature of solution dropped to lower temperature or raised to higher temperature.

Table 4.4

Solid phase Diffusion Coefficients and Film  
Transfer Coefficients for Phenol and PCP

adsorbate	temp(°C)	$D_S$ (cm <sup>2</sup> /sec)	$k_f$ (cm/sec)
phenol	20	$1.100 \times 10^{-8}$	$4.273 \times 10^{-3}$
	25	$2.888 \times 10^{-8}$	$4.634 \times 10^{-3}$
	30	$7.000 \times 10^{-8}$	$5.331 \times 10^{-3}$
	35	$1.300 \times 10^{-7}$	$5.818 \times 10^{-3}$
PCP	20	$1.521 \times 10^{-8}$	$4.602 \times 10^{-3}$
	25	$2.214 \times 10^{-8}$	$5.410 \times 10^{-3}$
	30	$4.478 \times 10^{-8}$	$6.326 \times 10^{-3}$
	35	$7.022 \times 10^{-8}$	$7.361 \times 10^{-3}$

Table 4.5

Solid phase Diffusion Coefficients and Film Transfer  
Coefficients Calculated from Equation 4.8 to 4.11

adsorbate	temp(°C)	$D_s$ (cm <sup>2</sup> /sec)	$k_f$ (cm/sec)
phenol	20	$1.155 \times 10^{-8}$	$4.227 \times 10^{-3}$
	25	$2.782 \times 10^{-8}$	$4.733 \times 10^{-3}$
	30	$6.507 \times 10^{-8}$	$5.280 \times 10^{-3}$
	35	$1.481 \times 10^{-7}$	$5.869 \times 10^{-3}$
PCP	20	$1.687 \times 10^{-8}$	$4.602 \times 10^{-3}$
	25	$2.902 \times 10^{-8}$	$5.409 \times 10^{-3}$
	30	$4.904 \times 10^{-8}$	$6.326 \times 10^{-3}$
	35	$8.147 \times 10^{-8}$	$7.362 \times 10^{-3}$



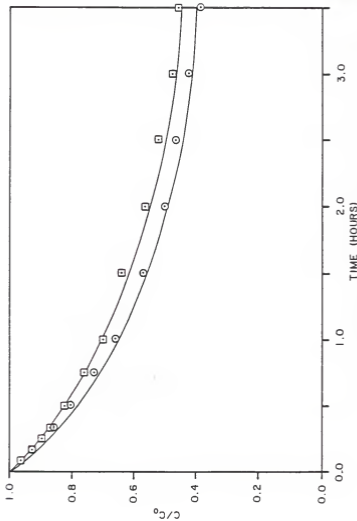


Figure 4.11 Adsorption Rates for Phenol at 20°C and 25°C.  
 ( □ 20°C, ○ 25°C, — model)

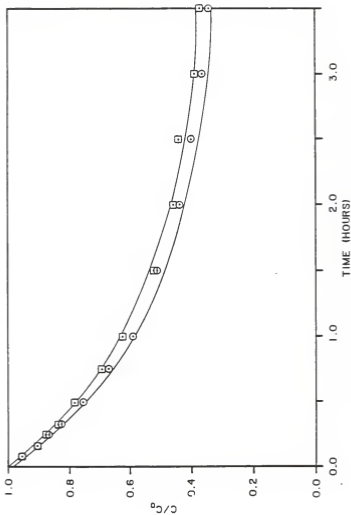


Figure 4.12 Adsorption Rates for Phenol at 30°C and 35°C.  
 ( □ 30°C, ○ 35°C; — model)

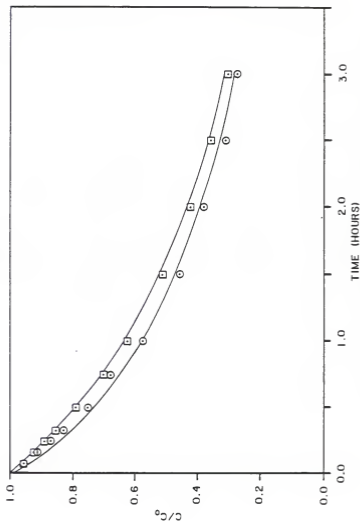


Figure 4.13 Adsorption Rates for PCP at 20°C and 25°C.  
 ( □ 20°C, ○ 25°C, — model)

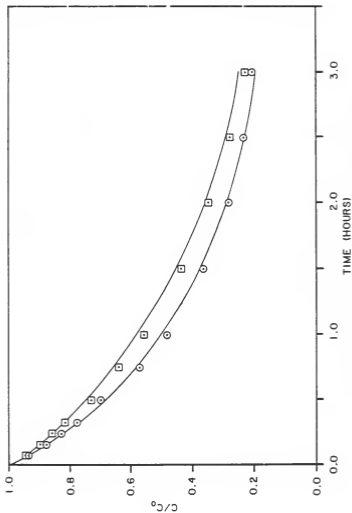


Figure 4.14 Adsorption Rates for PCP at 30°C and 35°C.  
(□ 30°C, ○ 35°C, — model)

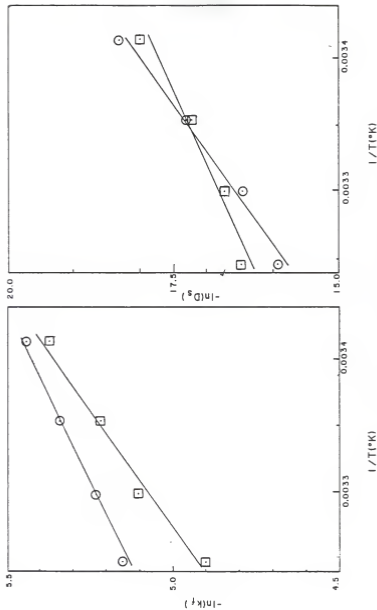


Figure 4.15  $k_f$  and  $D_g$  values versus  $T$  following Arrhenius' law  
 ( · □ phenol , ○ PGP )

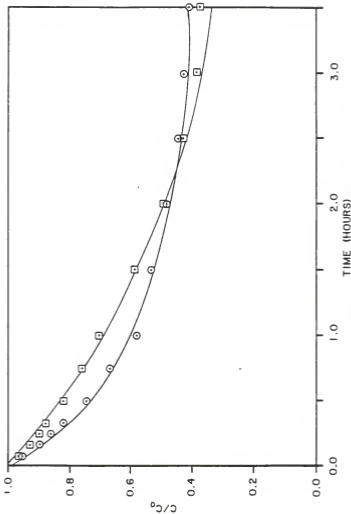


Figure 4.16 Adsorption Rates for Phenol for Step Change from 20°C to 35°C and from 35°C to 20°C after 1 hr (□ 20°C to 35°C, ○ 35°C to 20°C, — model)

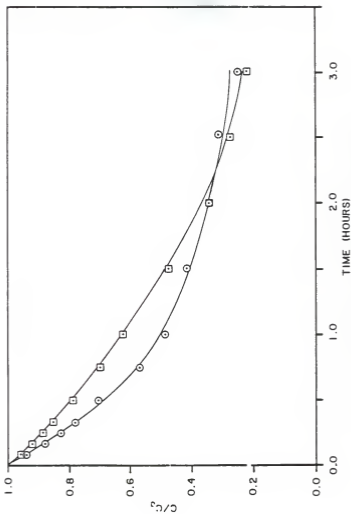


Figure 4.17 Adsorption Rates for PCP for Step Change from 20°C to 35°C and from 35°C to 20°C after 1 hr. ( $\square$  20°C to 35°C,  $\circ$  35°C to 20°C, — model)

#### 4-3 Fixed Bed Studies : Column

The experimental data obtained in the fixed bed tests were applied to judge the efficiency of the homogeneous solid phase diffusion model in predicting breakthrough curves. The operating data for the fixed bed experiments are listed from Tables 4.6 through 4.9. The input data for the fixed-bed program for predicting breakthrough curves include the isotherm parameters,  $k_f$  and  $D_p$ , total weight of carbon, diameter of particles, diameter of column, total flow rate, surface loading, influent concentration, and total bed height.

Breakthrough curves showing the plots of  $C/C_0$  versus time indicate the increase in the ratio of effluent to influent as adsorption in the column proceeds. The general pattern of the adsorption breakthrough curves, which exhibit like a characteristic S shape, are as expected for all fixed bed runs. After the trace of solute effluent was detected, the effluent concentration rose first gradually and then sharply till it approached the values of the influent concentration.

Figures 4.18 through 4.21 present experimental breakthrough data and the corresponding model prediction for phenol and PCP at temperatures of 20°C and 35°C. Comparison of the experimental and model predictions for these cases indicate that the model provides reasonable projections of the performance of fixed bed. From the breakthrough standpoint, it is better to operate the column at 20°C. Comparing  $C/C_0$  at 0.05, we see that the time for reaching  $C/C_0$  at 0.05 is 235 minutes at 20°C and 220 minutes at 35°C for phenol as well as for PCP 460 minutes at 20°C and 430 minutes at 35°C. The time for  $C/C_0$  reaching 0.10 is 270 minutes at 20°C and 250 minutes at 35°C for phenol and



310 minutes at 20°C and 450 minutes at 35°C for PCP.

The Adsorption capacity was higher at lower temperature from equilibrium experiments. But the adsorption rates increased with increased temperature as seen from batch kinetic experiments. These factors affecting adsorption give adverse influence on breakthrough curves. From the figures, it can be seen that  $C/C_0$  values at a temperature of 20°C are lower than those at 35°C at first half profile; however, the values are higher after that moment.

Step change experiments for the fixed bed studies were carried out for phenol and PCP at temperature from 20° to 35°C and from 35° to 20°C. A fixed bed program was modified by Mathews (1984) to take into account temperature change. Input data of the isotherm parameters, and the kinetic coefficients,  $K_f$  as well as  $D_p$ , were calculated from Equation 4.1 and from Equation 4.6 through Equation 4.9. The time of step change in temperature for the fixed bed experiments was after 3 hours and it took 30 minutes to raise the temperature from 20°C to 35°C. The input data for the isotherm parameters and  $K_f$  and  $D_p$  at 20°C was needed during initial 195 minutes. After that, the data of 35°C was applied to predict breakthrough curves.

Figures 4.22 through 4.25 show the experimental and predicted data of the breakthrough curves for phenol and PCP. Here, also, the modified program shows good predictions for all cases. It is apparent that the tests for step change from 20° to 35° show less adsorption than those from 35° to 20°C from comparing Figure 4.22 to 4.23 and Figure 4.24 to 4.25.

Table 4.6

## Operating Data for Fixed Bed Experiments at 20°C

	phenol	PCP
Total weight of carbon	75.0 gm	75.0 gm
Column diameter	3.1 cm	3.1 cm
Total bed height	23.2 cm	23.2 cm
porosity of bed	0.359	0.359
Influent concentration	194.12 mg/l	250.20 mg/l
Total flowrate	125.00 ml/min	125.00 ml/min
Surface loading	0.17 m <sup>3</sup> /min m <sup>2</sup>	0.17 m <sup>3</sup> /min m <sup>2</sup>
Dg <sup>a</sup> number	1188.29	1110.74
St <sup>b</sup> number	2.98	3.26
Bi <sup>c</sup> number	45.11	38.16

a.

Dg : Solute distribution parameter (dimensionless),  
 $Dg = \frac{P_0 Q_0 (1-\epsilon)}{\epsilon C_0}$   
 $P_0$  = adsorbent density including pore volume  
 $\epsilon$  = bed void fraction

b.

St : Stanton number (dimensionless),  $k_f \tau (1-\epsilon)/(R \epsilon \phi)$   
 $\tau$  = fluid residence time in fixed bed  
 $L/V$ ,  $V$  : interstitial fluid velocity, (L/v)  
 $\phi$  = sphericity, ratio of surface area of  
 equivalent-volume sphere to actual surface  
 area of adsorbent particle.

c.

Bi : Biot number based on solid phase diffusion  
 coefficient (dimensionless),  
 $k_f R (1-\epsilon)/(Dg D_s \epsilon \phi)$

Table 4.7

## Operating Data for Fixed Bed Experiments at 35°C

	phenol	PCP
Total weight of carbon	75.0 gm	75.0 gm
Column diameter	3.1 cm	3.1 cm
Total bed height	23.2 cm	23.2 cm
porosity of bed	0.359	0.359
Influent concentration	195.45 mg/l	243.78 mg/l
Total flowrate	125.00 ml/min	125.00 ml/min
Surface loading	0.17 m <sup>3</sup> /min m <sup>2</sup>	0.17 m <sup>3</sup> /min m <sup>2</sup>
Dg number	918.35	768.39
St number	4.06	4.06
Bi number	6.73	18.99

Table 4.8

## Operating Data for Fixed Bed Experiments :

Step Change from 20°C to 35°C after 3 hrs

	phenol	PCP
Total weight of carbon	75.0 gm	75.0 gm
Column diameter	3.1 cm	3.1 cm
Total bed height	23.2 cm	23.2 cm
porosity of bed	0.359	0.359
Influent concentration	194.12 mg/l	250.20 mg/l
Total flowrate	125.00 ml/min	125.00 ml/min
Surface loading	0.16 m <sup>3</sup> /min m <sup>2</sup>	0.16 m <sup>3</sup> /min m <sup>2</sup>
Dg number (20°C)	1278.42	976.92
(35°C)	990.71	840.58
St number (20°C)	3.07	3.35
(35°C)	4.27	5.35
Bi number (20°C)	29.40	38.54
(35°C)	5.52	14.83

Table 4.9

Operating Data for Fixed Bed Experiments :

Step Change from 35°C to 20°C after 3 hrs

	phenol	PCP
Total weight of carbon	75.0 gm	75.0 gm
Column diameter	3.1 cm	3.1 cm
Total bed height	23.2 cm	23.2 cm
porosity of bed	0.359	0.359
Influent concentration	195.45 mg/l	243.78 mg/l
Total flowrate	125.00 ml/min	125.00 ml/min
Surface loading	0.16 m <sup>3</sup> /min m <sup>2</sup>	0.16 m <sup>3</sup> /min m <sup>2</sup>
Dg number (35°C)	999.95	840.58
(20°C)	1290.35	976.92
St number (35°C)	4.27	5.35
(20°C)	3.07	3.35
Bi number (35°C)	5.47	14.83
(20°C)	39.14	38.54

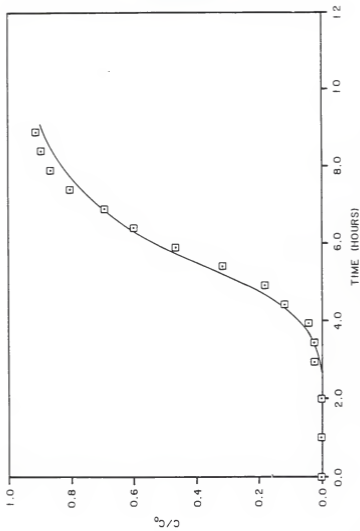


Figure 4.18 Breakthrough Curve for Phenol at 20°C.  
( □ exp, — model)

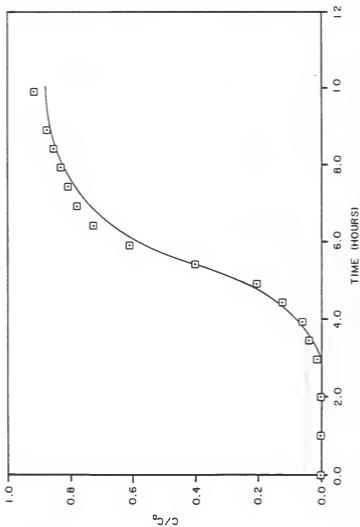


Figure 4.19 Breakthrough Curve for Phenol at 35°C.  
(□ exp, — model)

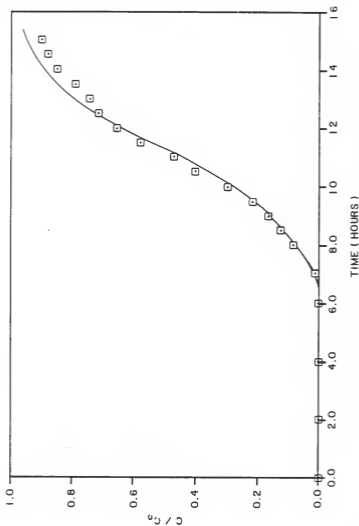


Figure 4.20 Breakthrough Curve for PCP at 20°C.  
 (  $\square$  exp , — model )



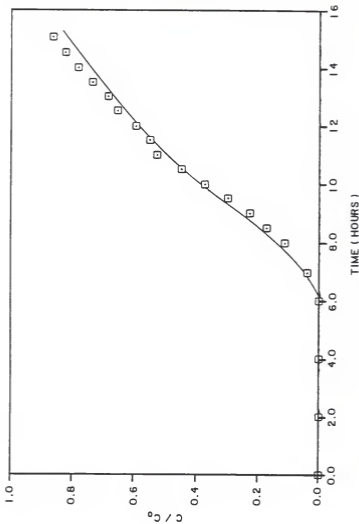


Figure 4.21 Breakthrough Curve for PCP at 35°C.  
 (  $\square$  exp , — model )

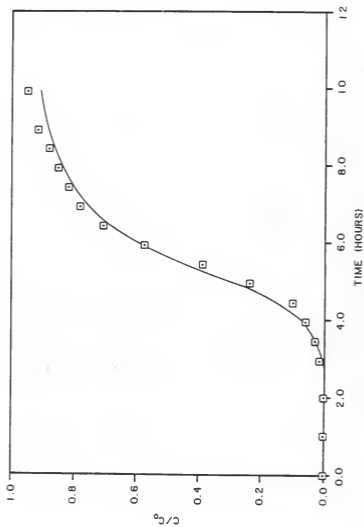


Figure 4.22 Breakthrough Curve for Phenol for Step Change from 20°C to 35°C after 3 hrs. .  
 ( □ exp , — model)

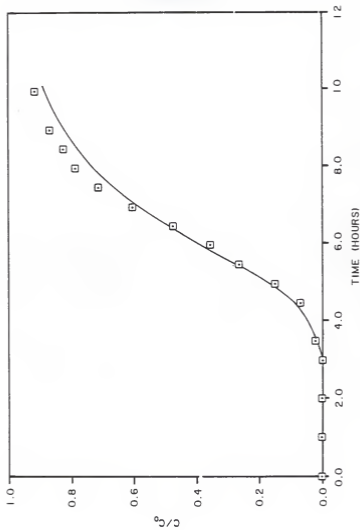


Figure 4.23 Breakthrough Curve for Phenol for Step Change from 35°C to 20°C after 3 hrs.  
(□ exp, — model)

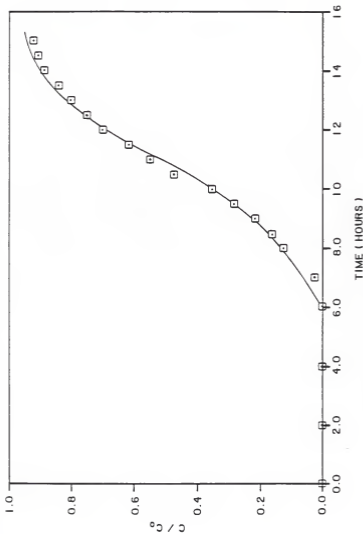


Figure 4.24 Breakthrough Curve for PCP for Step Change from 20°C to 35°C after 3 hrs.  
( □ exp , — model)

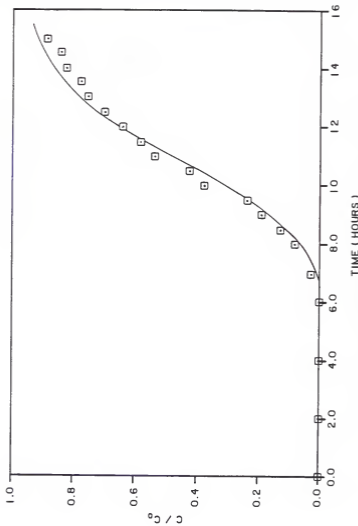


Figure 4.25 Breakthrough Curve for PCP for Step Change from 35°C to 20°C after 3 hrs.  
 ( □ exp , — model)

## CHAPTER 5.

### MULTICOMPONENT ADSORPTION

#### 5-1 Equilibrium Studies

In the multicomponent equilibrium studies, experimental data of a mixture of phenol and PCP were collected at 20°C and 35°C. Two models were selected to describe the bicomponent equilibrium system. They were :

1. Mathews' model (1975)

$$q_i = \frac{A_i (C_i/\eta_i)}{1 + \sum B_j (C_j/\eta_j)^{\beta_j}} \quad (2.31)$$

2. Prausnitz's model (IAS model)

The isotherm parameters, A, B, and  $\beta$ , used in both models are obtained from the single solute equilibrium studies.

In recent years, it becomes necessary to make use of theoretical models that allow the prediction of mixture equilibria from a minimum amount of experimental data. The comparison of these two models employing experimental data will be discussed to find efficiency of their predictions. Then, the models will be introduced to predict adsorption rates of multicomponent system which will be discussed in the next section.

Tables 5.1 and 5.2 list the experimental and predicted values of multicomponent equilibrium studies for Mathews' model and Prausnitz's model at 20°C. Tables 5.3 and 5.4 show the experimental and predicted values of both models at 35°C. The interaction coefficients,  $\eta_i$ , are obtained from mixture equilibrium data using single solute isotherm parameters, A, B, and  $\beta$ , developed for

each solute species in parameter estimation procedure. The values of  $\eta_1$  are 1.015 and 0.4113 for phenol at 20° and 35°C, respectively; whereas for PCP, those are 0.2095 and 0.1512.

For Mathews' model, the percent deviation are 26.6, 25.2 for phenol and 21.9, 20.7 for PCP at 20°C and 35°C, respectively. For Prausnitz's model, The values are 16.6, 15.8 for phenol and 13.1 12.4 for PCP at 20°C and 35°C, respectively. From The percent deviation standpoint, it can be seen that the surface concentration predictions by Prausnitz's model are in better conditions than Mathews' model.

Both models predict that PCP is adsorbed more strongly than phenol, which is evident from individual isotherms. The same results are proved that adsorption capacities are higher at lower temperature from both models.

It is not obvious to compare the results only from the data in Tables 5.1 to 5.4. The plots of  $q_{exp}/q_{calc}$  against the solution concentration for both models are illustrated in Figures 5.1 to 5.4 representing the Mathews' and Prausnitz's models for phenol and PCP at 20° and 35°C. For both temperatures, the prediction of Prausnitz's model is seen to be better than that of Mathews' model.

Table 5.1

Multicomponent Equilibrium for Phenol and PCP  
at 20°C by Mathews's Equilibrium Model

		Exp	Model	Exp	Model
C <sub>Phenol</sub>	C <sub>PCP</sub>	q <sub>Phenol</sub>	q <sub>Phenol</sub>	q <sub>PCP</sub>	q <sub>PCP</sub>
mmoles/l		mmoles/gm		mmoles/gm	
4.202	2.185	1.5190	1.4490	2.6550	1.9430
3.277	1.013	0.8547	1.8270	1.9750	1.3260
1.875	3.843 E-1	0.3180	0.2946	1.2490	0.7547
1.576	2.914 E-1	1.1440	1.2080	1.3940	1.1700
1.218	1.829 E-1	0.9440	0.9414	1.2020	0.7957
7.550 E-1	1.386 E-1	0.4360	0.5384	0.6860	0.5979
5.190 E-1	3.945 E-1	1.1700	1.0210	0.4740	0.3831
2.680 E-1	9.799 E-3	0.3740	0.4767	0.2310	0.1888
1.939 E-1	8.736 E-3	0.8800	0.6602	1.2350	0.8988
1.180 E-1	8.733 E-3	0.6100	0.7290	0.2387	0.2861
1.080 E-1	5.816 E-3	0.7120	0.6338	0.5010	0.4748
6.315 E-2	4.983 E-3	0.4930	0.5994	0.6240	0.4733
3.726 E-2	4.774 E-3	0.3090	0.2734	0.3330	0.3395
2.744 E-2	4.351 E-3	0.4800	0.3192	0.1920	0.2849
1.898 E-2	4.253 E-3	0.3320	0.2396	0.2490	0.3320
1.670 E-2	2.519 E-3	0.2490	0.2247	0.3570	0.4287
1.592 E-2	1.810 E-3	0.2500	0.1659	0.9900	0.9717
3.280 E-3	9.370 E-4	0.0567	0.5340	0.6520	0.5496



Table 5.2

Multicomponent Equilibrium for Phenol and PCP  
 at 20°C by Prausnitz's Equilibrium Model

		Exp	Model	Exp	Model
C <sub>Phenol</sub>	C <sub>PCP</sub>	q <sub>Phenol</sub>	q <sub>Phenol</sub>	q <sub>PCP</sub>	q <sub>PCP</sub>
moles/l		moles/ga		moles/ga	
4.202	2.185	1.5190	1.9660	2.6550	2.4630
3.277	1.013	0.8547	0.6549	1.9750	1.8700
1.875	3.843 E-1	0.3180	0.2934	1.2490	1.3807
1.576	2.914 E-1	1.1440	1.1730	1.3940	1.4770
1.218	1.829 E-1	0.9440	0.9906	1.2020	1.3760
7.550 E-1	1.386 E-1	0.4360	0.4560	0.6860	0.6083
5.190 E-1	3.945 E-1	1.1700	1.1380	0.4740	0.3376
2.680 E-1	9.799 E-3	0.3740	0.2992	0.2310	0.2063
1.939 E-1	8.736 E-1	0.8800	0.9241	1.2350	1.3180
1.180 E-1	8.733 E-3	0.6100	0.5152	0.2387	0.2087
1.080 E-1	5.816 E-3	0.7120	0.7890	0.5010	0.4792
6.315 E-2	4.983 E-3	0.4930	0.4772	0.6240	0.5105
3.726 E-2	4.774 E-3	0.3090	0.4236	0.3330	0.3220
2.744 E-2	4.351 E-3	0.4800	0.3828	0.1920	0.1438
1.898 E-2	4.253 E-3	0.3320	0.3167	0.2490	0.2136
1.670 E-2	2.519 E-3	0.2490	0.2938	0.3570	0.2919
1.592 E-2	1.810 E-3	0.2500	0.2577	0.9900	0.9393
3.280 E-3	9.370 E-4	0.0567	0.0780	0.6520	0.4227

Table 5.3

Multicomponent Equilibrium for Phenol and PCP  
at 35°C by Mathews's Equilibrium Model

		Exp	Model	Exp	Model
CPhenol	CPCP	qPhenol	qPhenol	qPCP	qPCP
moles/l		moles/g <sub>m</sub>		moles/g <sub>m</sub>	
3.887	2.153	1.5030	1.0000	1.6920	1.4250
3.009	1.272	0.8860	0.6324	1.1220	1.0700
1.695	7.363 E-1	0.3660	0.2799	1.3420	0.7959
1.383	2.972 E-1	0.8723	0.8681	1.3080	0.7228
1.187	2.714 E-1	0.7990	0.7203	0.8670	0.8398
1.141	2.443 E-1	0.9100	0.8617	0.7910	0.6146
6.195 E-1	1.897 E-1	0.4510	0.4783	1.3350	0.5742
4.928 E-1	1.003 E-1	1.0650	1.0890	0.8614	0.7489
3.265 E-1	5.163 E-1	0.7420	0.7779	0.9620	0.6462
2.437 E-1	5.010 E-2	0.8290	0.5934	0.4260	0.4889
1.794 E-1	3.994 E-2	0.5760	0.7159	0.7710	0.6627
1.791 E-1	3.876 E-2	0.6710	0.7281	0.4150	0.3701
1.771 E-1	3.115 E-2	0.3740	0.3300	0.5500	0.5133
9.925 E-2	2.261 E-2	0.2901	0.3100	0.5690	0.2003
9.963 E-2	2.210 E-2	0.4680	0.3973	0.3670	0.4754
6.794 E-2	1.863 E-2	0.3140	0.3464	0.3890	0.2979
4.998 E-2	1.803 E-2	0.2380	0.2095	0.3400	0.2920
2.954 E-2	1.519 E-3	0.4580	0.2898	0.5160	0.5011
2.442 E-2	9.675 E-3	0.1600	0.2010	0.2270	0.3803

Table 5.4

Multicomponent Equilibrium for Phenol and PCP  
at 35°C by Prausnitz's Equilibrium Model

CPhenol		CPCP		Exp	Model	Exp	Model
mnoles/l		mnoles/gm		QPhenol	QPhenol	QPCP	QPCP
3.887	2.153	1.5030	1.3600	1.6920	2.1690		
3.009	1.272	0.8860	0.6794	1.1220	1.3140		
1.695	7.363 E-1	0.3660	0.3256	1.3420	1.2730		
1.383	2.972 E-1	0.8723	0.8307	1.3080	0.9451		
1.187	2.714 E-1	0.7990	0.8897	0.8670	1.3280		
1.141	2.443 E-1	0.9100	1.2070	0.7910	0.5319		
6.195 E-1	1.897 E-1	0.4510	0.4138	1.3350	1.4750		
4.928 E-1	1.003 E-1	1.0650	0.9467	0.8614	0.5982		
3.265 E-1	5.163 E-1	0.7420	0.9301	0.9620	1.1950		
2.437 E-1	5.010 E-2	0.8290	0.7987	0.4260	0.3756		
1.794 E-1	3.994 E-2	0.5760	0.4865	0.7710	0.6178		
1.791 E-1	3.876 E-2	0.6710	0.7756	0.4150	0.3167		
1.771 E-1	3.115 E-2	0.3740	0.3822	0.5500	0.4098		
9.925 E-2	2.261 E-2	0.2901	0.3063	0.5690	0.6266		
9.963 E-2	2.210 E-2	0.4680	0.5307	0.3670	0.2093		
6.794 E-2	1.863 E-2	0.3140	0.4575	0.3890	0.2782		
4.998 E-2	1.803 E-2	0.2380	0.3228	0.3400	0.2782		
2.954 E-2	1.519 E-3	0.4580	0.3002	0.5160	0.4092		
2.442 E-2	9.675 E-3	0.1600	0.2398	0.2270	0.1524		

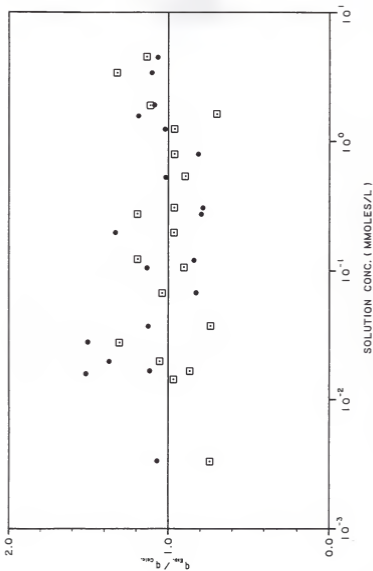


Figure 5.1 Phenol in Multicomponent Isotherm at 20°C.  
 (  $\square$  Mathews' model,  $\bullet$  Prausnitz's model)

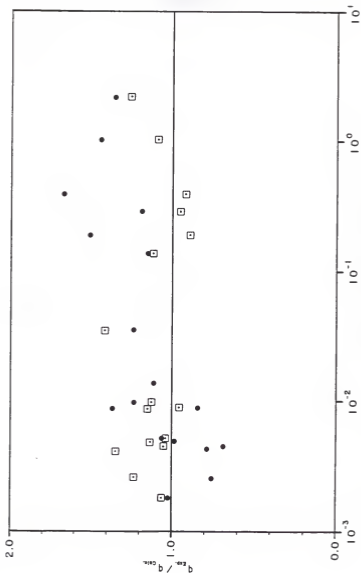


Figure 5.2 PCP in Multicomponent Isotherm at 20°C.  
 (  $\square$  Mathews' model,  $\bullet$  Prausnitz's model)

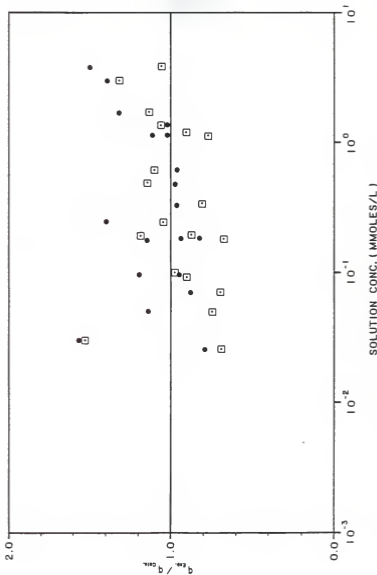


Figure 5.3 Phenol in Multicomponent Isotherm at 35°C.  
 (□ Mathews' model, ● Prausnitz's model)

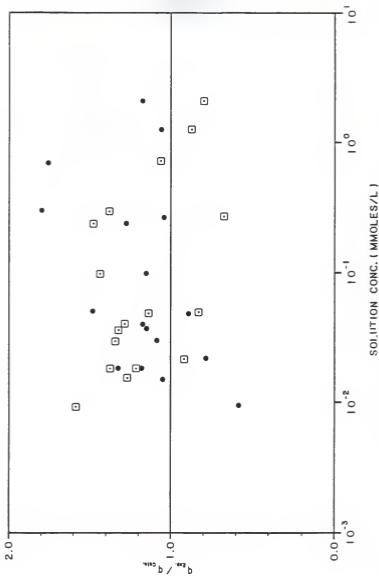


Figure 5.4 PCP in Multicomponent Isotherm at 35°C.  
 (  $\square$  Mathews' model,  $\bullet$  Prausnitz's model)

## 5-2 Batch Kinetic Studies

Four runs with two constant temperatures, 20°C and 35°C, and two step changes, from 20°C to 35°C and from 35°C to 20°C, were conducted for batch kinetic studies of multicomponent solution. The operating conditions were the same as in single solute batch reactions as discussed in section 4-2. Carbon size of 20/25, stirring speed of 700 rpm, reaction volume of 24 liters solution made up of tap water, total carbon weight of 6 gm, and pH value at 7 were used for all batch kinetic multicomponent experiments. The initial concentration of the solutions included  $2.5 \times 10^{-4}M$  phenol and  $2.5 \times 10^{-4}M$  PCP.

Adsorption rates for constant temperature were predicted by using the computer program developed by Mathews (1975). The data of both Mathews' and Prausnitz's equilibrium models were used in the computer program separately. Figures 5.5 and 5.6 depict the results with Mathews' equilibrium model at 20°C and 35°C; Figures 5.7 and 5.8 show the results with Prausnitz's equilibrium model.

For Prausnitz's model in predicting adsorption rates, the percent deviation between the experimental and predicted data are 2.58 for phenol and 16.89 for PCP at 20°C as well as 5.82 for phenol and 19.85 for PCP at 35°C. For Mathews' model, the values are 4.95 for phenol and 9.43 for PCP at 20°C as well as 6.00 for phenol and 10.62 for PCP at 35°C. Both models gave reasonable predictions. It seems that adsorption rate model using Prausnitz's equilibrium correlation does not give as good a prediction as the Mathews' model.

For step change experiments, adsorption rates were predicted by using rate model incorporating the Prausnitz's equilibrium models. A modification of the



computer program incorporating Prausnitz's equilibrium model developed by Mathews (1984) was used to predict kinetic curves for change in temperature, similar to previous sections. The result of adsorption rate for step change from 20°C to 35°C is represented in Figure 5.9. The percent deviations between the predicted and experimental data are 4.29 for phenol and 20.32 for PCP. It took 20 minutes for the temperature of solution to drop from 35°C to 20°C. In predicting adsorption rates from 35°C to 20°C, the result give as reasonable agreement as can be seen from Figure 5.10. The percent deviations are 9.90 for phenol and 9.18 for PCP. The possible explanation of the difference between experimental and predicted data is that the procedure of adding dry ice to decrease the temperature affect the stirring speeds and induces vaporization of adsorbates.

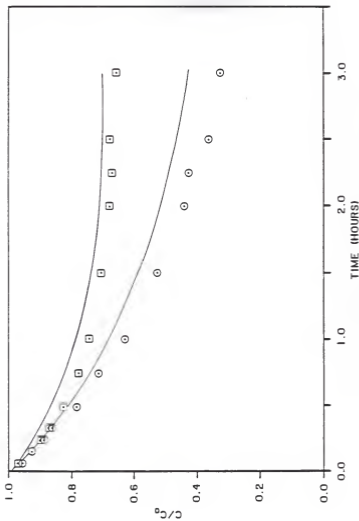


Figure 5.5 Adsorption Rates for (Phenol + PCP) at 20 C  
with Prausnitz's Equilibrium Model.  
(  $\square$  Phenol,  $\circ$  PCP, — model)

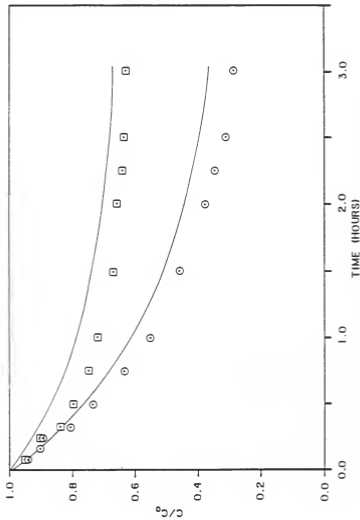


Figure 5.6 Adsorption Rates for (Phenol + PCP) at 35 C with Mathews' Equilibrium Model.  
 (  $\square$  Phenol ,  $\circ$  PCP , — model)

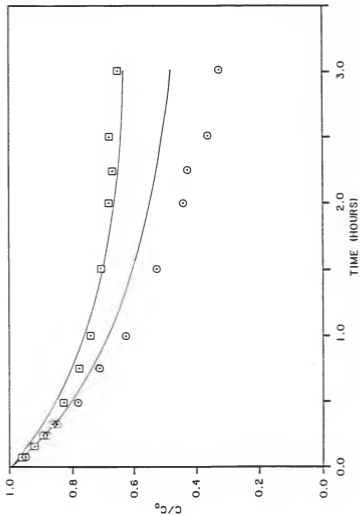


Figure 5.7 Adsorption Rate for (Phenol + PCP) at 20°C  
with Prausnitz's Equilibrium Model.  
(  $\square$  Phenol,  $\circ$  PCP, — model)

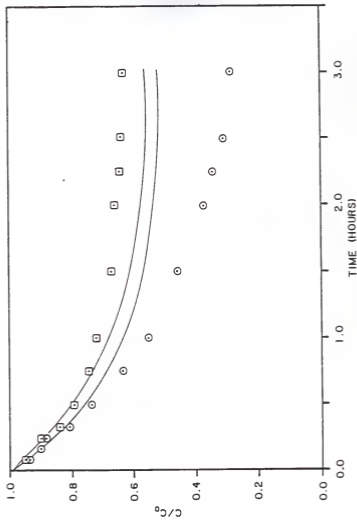


Figure 5.8 Adsorption Rate for (Phenol + PCP) at 35°C with Prausnitz's Equilibrium Model. (  $\square$  Phenol,  $\circ$  PCP, — model)

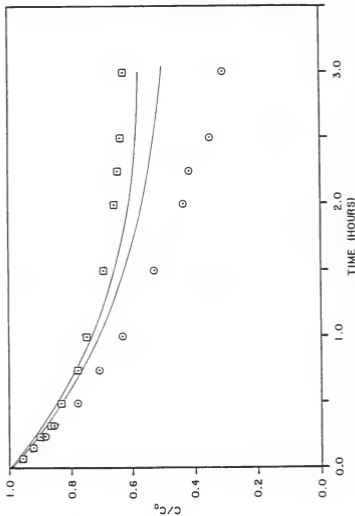


Figure 5.9 Adsorption Rate for (Phenol + PCP) for Step Change from 20°C to 35°C with Prausnitz's Model.  
 ( □ Phenol , ○ PCP , — model)

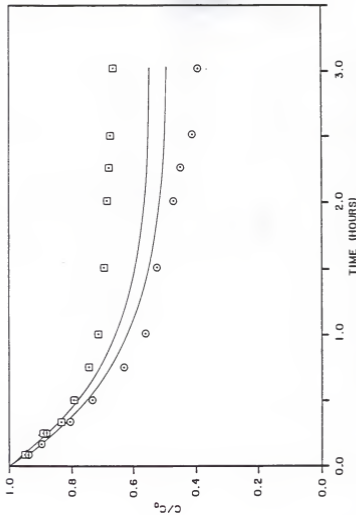


Figure 5.10 Adsorption Rate for (Phenol + PCP) for Step Change from 35°C to 20°C with Praunnitz's Model.  
 ( □ Phenol, ○ PCP, — model)

### 5-3 Fixed Bed Studies

Two runs were made in the fixed bed experiments with multicomponents solutions, i.e., step changes from 20°C to 35°C and from 35°C to 20°C after 3 hours. The total flowrate and total weight of carbon used in two runs were the same as those in the single solute studies. The breakthrough curves of two runs were obtained from conducting multicomponent solution consisting  $1 \times 10^{-3}M$  of phenol and  $2 \times 10^{-3}M$  of PCP as initial concentration. The runs were terminated till the  $C/C_0$  values of PCP approaching 0.95. The duration of experiments was 12 hours.

Figure 5.11 shows the experimental data of the step change experiments from 20° to 35°C; while Figure 5.12 depicts the data from 35° to 20°C. The reason for  $C/C_0$  values of phenol greater than 1 is because of displacement of previously adsorbed phenol by PCP and elution of phenol into liquid phase. The amount of phenol displaced by PCP reached maximum at the highest points shown in the plots. After the peak, the displacement became slower and the values of  $C/C_0$  of phenol decreased as time progressed.

From the plots, it can be seen that for phenol, the  $C/C_0$  values for step change from 35°C to 20°C were greater than those from 20°C to 35°C; while for PCP, the values from 35°C to 20°C were less than those from 20°C to 35°C. The mechanisms and phenomenon of the multicomponent fixed bed adsorption for step change in temperature are very complex because the time for changing temperature is also a variable affecting adsorption profiles. The observation of variables on multicomponent fixed bed adsorption is not within the scope of this research. Further investigations are recommended on this point.



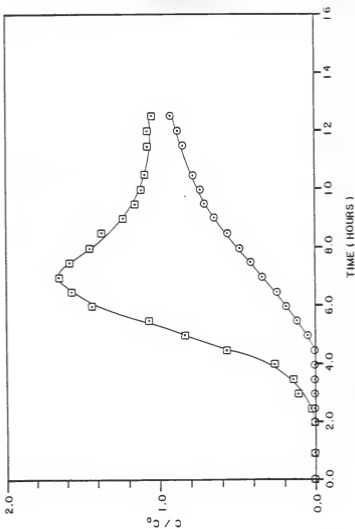


Figure 5.11 Breakthrough Curves for (Phenol + PCP) for Step Change from 20°C to 35°C after 3 hrs.  
 ( —□— Phenol, —○— PCP )

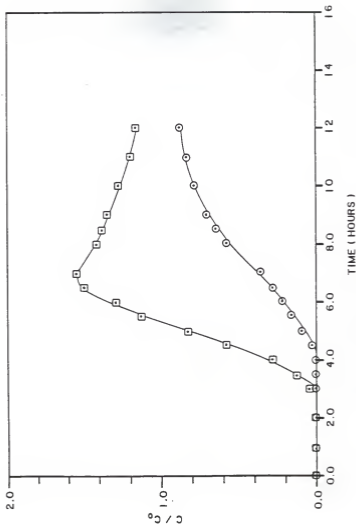


Figure 5.12 Breakthrough Curves for (Phenol + PCP) for Step Change from 35°C to 26°C after 3 hrs.  
 (—○— Phenol, - -□- PCP)

## CHAPTER 6.

### CONCLUSIONS AND RECOMMENDATIONS

#### 6-1 Conclusions

1. Temperature affects both adsorption capacity from equilibrium experiments and adsorption rates from batch kinetic experiments.
2. The three parameter equation described adsorption capacity well for both phenol and PCP at four different temperatures. The extended three parameter equation was developed to show the temperature effect on capacity based on data at four temperatures.
3. The homogeneous solid phase diffusion model described satisfactorily adsorption rates of single solute with constant temperature. The values of  $k_f$  and  $D_s$  obtained from the batch kinetic model were correlated with temperature based on the Arrhenius' law. The modified kinetic model was tested for runs with step changes from 20°C to 35°C and 35°C to 20°C and showed good capability for predicting adsorption rate.
4. The fixed-bed program based on the homogeneous solid phase diffusion model was used to predict breakthrough curves of phenol and PCP at 20°C and 35°C. The operation of this fixed bed at 20°C was found to be better than at 35°C from the breakthrough curves. The modified fixed-bed program used in predicting breakthrough curves for step changes was found to provide excellent prediction.

5. Both Mathews' model and Prausnitz's model gave reasonable estimation for multicomponent equilibria. However, accuracy of multicomponent rate model predictions seems to be limited by the inability to predict mixture equilibria satisfactorily.
6. In the adsorption rates studies for multicomponent solution, the adsorption rate model based on IAS model provide good prediction for runs with constant temperature. In addition, the rate model which was modified to include temperature changes gave predictions in moderately good agreement for runs with step change in temperature.
7. Experimental results from multicomponent breakthrough curves showed that the  $C/C_0$  values of phenol for step change from 35°C to 20°C were greater than those of from 20°C to 35°C; while the values of PCP for step change from 35°C to 20°C were less than those of from 20°C to 35°C.

## 6-2 Recommendations

1. Extend the application of the modified three parameter equation, which is available for several temperature, to other priority pollutants and test with other ranges of temperatures.
2. The rate model and the fixed-bed model were found in good agreement in predicting adsorption rates and breakthrough for a single solute of phenol and PCP. Extend the application of the models and test the efficiency with other priority pollutants.
3. The modified models for studying step change can be extended to take into account time as a variable, i.e., changing temperature at different times to test the efficiencies of the models in predicting batch kinetic data or breakthrough curves. The model can be verified by running experiments and calculating predictive data, which were conducted with testing different priority pollutants, changing temperature at different time, and step change with different temperature.

#### REFERENCES

- Benefield, L. D. and Jodkins, J. F. and Weand, B. L. (1982). Process Chemistry for Water and Wastewater Treatment
- Bulter, J. A. V. and Ockrent, C. (1930). Studies in Electrocapillarity. III. J. Phys. Chem. 34, 2841.
- Crittenden, J. C. and W. J. Weber, Jr. (1978a). Predictive Model for Design of Fixed Bed Adsorbers : Parameter Estimation and Model Development. J. Env. Eng. Div. ASCE, 104, 185.
- Crittenden, J. C. and W. J. Weber, Jr. (1978b). Predictive Model for Design of Fixed Bed Adsorbers : Single Component Model Verification. J. Env. Eng. Div. ASCE, 104, 433.
- Crittenden, J. C. and W. J. Weber, Jr. (1978c). Model for Design of Multicomponent Adsorption System. J. Env. Eng. Div. ASCE, 104, 1175.
- Crittenden, J. C. and Wong, B. W. C. and Thacker, W. E. and Snoeyink, V. L. and Hinrichs, R. L. , (1980) Mathematical Model of Sequential Loading in Fixed-Bed Adsorbers. J. Water Poll. Control Fed. 52, 2780.
- Danner, P. Ronald (1983). Application of Vacancy Solution Theory to Gas Adsorption The Pennsylvania State University
- DiGiano, F. M. and Weber, Jr. W.J. (1972) Sorption Kinetics in Finite-batch Systems. Proc. Am. Soc. of Civ. Engr. Saint. Eng. Div. 98, SA6, 1020.
- Edeskuty, F. J. and Amundson, N. R. (1952) Mathematics of Adsorption IV. Effect of Intraparticle diffusion in Agitated Static Systems. J. Phys. Chem. 56, 148.
- Fasularo, J. and Mueller, J. A. and Pennu, A. S. (1980). Prediction of Carbon Column Performance from Pure-Solute J. Water Poll. Control Fed. V.52 P.2019.
- Freundlich, H. (1926). Colloid and Capillary Chemistry, Methuen and Co., Ltd., London.
- Friedel, R. A. and Orchin, M. (1951). Ultraviolet Spectra of Aromatic Compounds. John Wiley and Sons, Inc.
- Glueckauf, E. (1955). Theory of Chromatography, Part 10 --- Formulae for Diffusion into Spheres and Their Application to Chromatography. Trans. Faraday Soc. 51, 2019.

- Hand, D. W. , and Crittenden, J. C. , and Thacker, W. E., (1984). Simplified Models for Design of Fixed Bed Adsorption Systems. J. Env. Eng. Div. ASCE , 110, 441.
- Jossens, L. Prausnitz, W. F. , Schlunder, E. U. and Myers, A. L. (1978). Thermodynamics of Multisolute Adsorption from Dilute Aqueous Solution. Chem. Eng. Sci., 33, 1097.
- Kesten, P. R. and Laoidus, L. and Amundson, N. R. (1952) Mathematics of Adsorption in Beds. V. Effect of Intraparticle Diffusion in Flow System in Fixed-bed Adsorbers. J. Phys. Chem. 56, 683
- Keith, L. H. and Telliard, W. A. (1979). Priority Pollutants I-a perspective view. Env. Sci. and Tech. 13, 416.
- Khan, K. A. and Suidan, M. T. and Cross, W. H. (1981). Anaerobic Activated Carbon Filters for the Treatment of Phenol-Bearing Wastewater. J. Water Poll. Control Fed., 53, 1519.
- Langmuir, J. (1918). The Adsorption of Gases on Planes of Glass, Mica and Platinum. J. Amer. Chem. Soc., 40, 1361.
- Lee, M. C. and Crittenden, J. C. and Snoeyink, V. L. and Ari, M. (1983) Design of Carbon Beds to Remove Humic Substance. J. Env. Eng. Div. ASCE, 109, 631.
- Letterman, R. and Quon, J. E. and Gessell, R. S. (1974). Film Transport Coefficients in Agitated Suspensions of Activated Carbon. J. Water Poll. Control Fed., 46, 2536.
- Lispis, A. I. and Rippen, D. W. T. (1977). A General Model for the Simulation of Multicomponent Adsorption from a Finite Bath. Chem. Eng. Sci. 32, 619.
- Lispis, A. I. and Rippen, D. W. T. (1978). The Simulation of Binary Adsorption in Activated Carbon Columns Using Estimated of Diffusional Resistance within the Carbon Particles Derived from Batch Experiments. Chem. Eng. Sci., 33, 593.
- Lispis, A. I. and Roppen, D. W. T. (1979). The Simulation of Binary Adsorption in Continuous Countercurrent Operation and a Comparison with Other Operating Models. Amer Inst. Chem. Eng. Sci. 25, 455.
- Liu, K. T. and Weber, W. J. Jr. (1981). Characterization of Mass Transfer Parameters for Adsorbers Modeling and Design. J. Water Poll. Control Fed. 53, 1541.
- Mansour, A and Von Rosenberg, D. L. and Sylvester, N. D. (1982). Numerical Solution of Liquid-Phase Multicomponent Adsorption in Fixed Beds Amer. Inst. Chem. Eng. J. 28, 765.

- Markham, F. D. and Benton, A. F. (1931). J. Amer. Chem. Soc. 53, 497.
- Martin, R. J. and Al-Bahrani. (1976). Adsorption Studies Using Gas Liquid Chromatography - I Effect of Molecular Structure. Water Research, 10, 731.
- Martin, R. J. and Al-Bahrani. (1977). Adsorption Studies Using Gas Liquid Chromatography - II Competitive Adsorption. Water Research. 11, 991.
- Martin, R. J. and Al-Bahrani. (1978). Adsorption Studies Using Chromatography - III Experimental Factors Influencing Adsorption Water Research. 12, 879.
- Masamune, S. and J. M. Smith (1965). Adsorption Rate Studies - Interaction of Diffusion and Surface Processes. Amer. Inst. Chem. Eng. J., 11, 34.
- Mathews, A. P. and Weber W. J., Jr. (1977). Effects of External Mass Transfer and Intraparticle Diffusion on Adsorption Rates in Slurry Reactors. Amer. Inst. Chem. Eng. Symp. Ser. 73, 91.
- Mathews, A. P. and Weber W. J., Jr. (1984). Modeling and Parameter Evaluation for Adsorption in Slurry Reactors Chem. Eng. Commun. V.25, P.157.
- Mathews, A. P. and Su, C. A. (1983). Adsorption Kinetics of Two Priority Pollutants. Environmental Progress, 2, 257.
- Mathews, A. P. (1984). Unpublished work. Department of Civil Engineering, Kansas State University.
- Merk, W. and Fritz, W. and Schlunder, E. L. (1981). Competitive Adsorption of Two Dissolved Organics onto Activated Carbon -- III Adsorption Kinetics in Fixed Beds. Chemical Engr. Sci. 36, 743.
- Myers, A. L. and Prausnitz, J. M. (1965). AIChE J., V.11, p.121.
- Motoyuki Suzuki and Takao Fujii (1982). Concentration Dependence of Surface Diffusion Coefficient of Propionic Acid in Activated Carbon Particles. AIChE 28, 380.
- Narbaiz, R. M. and Benedek, A. (1983). Least Cost Process Design for Granular Activated Adsorbers. J. Water. Poll. Control. Fed. V.55, No.10, P.1244.
- National Research Council (1980). Drinking Water and Health, Vol.2. Nat. Academy Press, Wash. D. C.
- Peel, R. G. and Benedek, A. (1980). Dual Rate Kinetic Model of Fixed Bed Adsorber. J. Env. Eng. Div. ASCE. 106, 797.



- Pirbazeri, M and Weber W. J., Jr. (1982). Adsorption of Toxic and Carcinogenic Compound from Water. J. AWWA, 74, 203.
- Pirbazeri, M and Weber W. J., Jr. (1984). Adsorption of P-Dichlorobenzene from Water. J. AWWA, 76, 82.
- Radke, C. J. and Prausnitz, J. M. (1972a). Thermodynamics of Multi-Solute and Adsorption from Dilute Liquid Solution. Amer. Inst. Chem. Eng. J., 18, 176.
- Radke, C. J. and Prausnitz, J. M. (1972b). Adsorption of Organic Solute from Dilute Aqueous Solution On Activated Carbon. Ind. Eng. Chem. Fund., 11, 145.
- Redlich, O. and Peterson, C (1959). J. Phys. Chem. 63, 1024.
- Rosen, J. B. (1952). Kinetics of a Fixed-Bed System for Solid Diffusion into Spherical Particles. J. Chem. Phys. 20, 387.
- Strudgeon, G. E. and Lewis, B. J. and Albary, W. W. and Clinger, R. C. (1980). Safety Consideration in Handling Activated Carbon. J. Water Poll. Control Fed., 52, 2516.
- Sudo, Y., D. M. Mistic and M. Suzuki (1978). Concentration Dependence of Effective Surface Diffusion Coefficients in Aqueous Phase Adsorption on Activated Carbon. Chem. Eng. Sci. 33, 1267.
- Suzuki, M and K. Kawazoe (1975). Effective Surface Diffusion Coefficients of Volatile Organics on Activated Carbon During Adsorption from Aqueous Solution J. Chem. Eng. Japan 8, 379.
- Tien, C. and Hsieh, J. S. C. and Turian, R. M. (1976). Application of h-Transformation for the Solution of Multicomponent Adsorption in Fixed-Bed. Amer. Inst. Chem. Engr. J. 22, 498.
- Tien, C. (1981). Recent Progress in the Calculation of Multicomponent Adsorption in Fixed Beds. present at 181st Am. Chem. Soc. National meeting Atlanta, Georgia.
- Weber, W. J. Jr. and Voice, T. C. and Jodallah, A. (1983). Adsorption of Humic Substance : Effects of Heterogeneity and System Characteristics. J. AWWA 75, 612.
- Van Vliet B. M. and W. J. Weber, Jr. (1980). Modeling and Prediction of Specific Compound Adsorption by Activated Carbon. Water Research, 14(12), 1719.
- Van Vliet B. M. and W. J. Weber, Jr. (1981). Comparative Performance of Synthetic Adsorbents and Activated Carbon for Specific Compound Removal from Wastewater. J. Water Poll. Control Fed. 53, 1585.

- Verseulean, T. (1953). Theory for Irreversible and Constant Pattern Solid Diffusion. Ind. Eng. Chem. Fund., 45, 1664.
- Villadsen, J. W. and R. K. Chakravorti (1974). Pore and Surface Diffusion Models for Fixed Bed Adsorption. Amer. Inst. Chem. Eng. J., 20, 226.
- Westersark, Mats (1975). Kinetics of Activated Carbon Adsorption J. Water Poll. Control Fed., 47, 704.
- Wilson, J. N. (1940). A Theory of Chromatography. J. Amer. Chem. Soc., 62, 1583.
- Wilde, K. A. (1980). Multicomponent Adsorption Column Parameter Studies in Activated Carbon Adsorption. Vol.1, Ed, I. H. Suffet and M. J. McGuire, Ann Arbor Science Publisher, Ann Arbor, Michigan, p.251.
- Yen, Chen-Yu and Singer, P. C. (1984). Competitive Adsorption of Phenols on Activated Carbon. J. Env. Eng. Div., ASCE, 110, 976.

TEMPERATURE EFFECTS ON ACTIVATED  
CARBON ADSORPTION IN FIXED-BEDS

by

IE-HONG LIN

B.E., National Chang Kung University  
Taiwan, R.O.C. , 1980

---

AN ABSTRACT OF A MASTER'S THESIS

submitted in partial fulfillment of the

requirements for the degree

MASTER OF SCIENCE

Department of Civil Engineering

KANSAS STATE UNIVERSITY  
Manhattan, Kansas

1985

## ABSTRACT

A mathematical model of fixed bed adsorption was modified to take into account temperature as a variable. The model was employed to compare the performance of fixed beds at constant temperature and step changes in temperature. The equations which include the kinetic coefficients, film transfer and solid phase diffusion in particle, and adsorption capacity as variables were solved by orthogonal collocation methods.

Phenol and parachlorophenol (PCP) were used as adsorbates. Four constant temperatures, 20°, 25°, 30°, and 35°C, as well as two temperature step change, from 20° to 35°C and, from 35° to 20°C were tested. For single solute, isotherms at four temperatures were conducted. An equation is developed to show temperature effect on capacity based on data at four different temperatures. Batch kinetic studies were carried out at four temperatures and two step changes. Film transfer and solid phase diffusion coefficients obtained from batch kinetic model were correlated with temperature. The correlated film transfer and solid phase diffusion coefficients were used to predict adsorption rates for step changes in temperature. For multicomponent, equilibrium and batch kinetic studies were accomplished for temperatures of 20° and 35°C. Mathews' and Prausnitz's models were adopted to fit the experimental data. But only Prausnitz's model was modified to predict the batch runs with step change because of its more accuracy in describing constant temperature tests.

In fixed bed runs, experimental data were tested against the mathematical model with 20° and 35°C. For step change tests, the modified model using

variables from extended isotherms and correlated  $K_f$ ,  $D_s$  was applied in predicting breakthrough profile. Multicomponent adsorption in fixed beds for step change in temperature were conducted to compare breakthrough profile of each solute.